

## CHAPTER 1

### INTRODUCTION

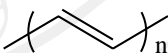
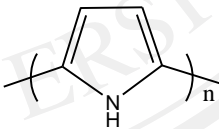
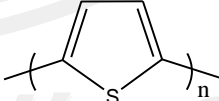
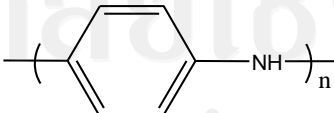
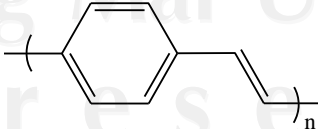
There are seven parts in this chapter consisting of the background of conducting polymers (CPs), cyclic voltammetry (CV), surface plasmon resonance spectroscopy (SPR) technique, some biomolecules (such as catecholamine (CA), uric acid (UA) and ascorbic acid (AA)), single-wall carbon nanotubes (SWNTs), ZnO nanoparticles and literature review.

#### 1.1 Conducting polymers[1–10]

Conducting polymers (CPs) are the exciting new class of electronic materials so called the intrinsically conductive polymer (ICPs) or electroactive polymer. The CPs have both electrical and optical properties plus a high conductivity, which can be changed by simple oxidation or reduction [1]. In 1967, a postgraduated student of Shirakawa at Tokyo Institute of Technology synthesized the polyacetylene using Ziegler-Natta catalysts, and a silvery thin film was produced by mistake. When this material under investigation the property was found similar to that of semiconductor. Polyacetylene was doped by oxidation with halogen (iodine) referred to as p-doping or/and reduction with alkaline metal (sodium) as n-doping. In 1977, MacDiarmid et al. reported the large increase in conductivity of polyacetylene after doping with iodine that the first of ICPs was recognized, and the team received the Nobel Prize in Chemistry in 2000 [2]. The CPs have the potential of combining the high conductivity

of pure metals with the processability and good corrosion stability when contract with solution or/and in the dry state. Furthermore, they have many field applications, depending on the specific ionic and electronic resistances, such as polymer battery [3], electrochromic displays [4], light emitting diodes [5], and biosensor [6–9]. The CPs such as polypyrrole, polythiophene, polyaniline and their derivatives are used for biosensor application. Polyaniline (PANI) has been extensively studied polymer due to its high electrical conductivity, environmental stability and ease synthesize [10, 11]. Chemical structures of some of the most common conjugated polymers are shown in Table 1.1 [1, 12]. Conjugated polymers derive their semiconducting properties by having delocalized  $\pi$ -electron bonding along the polymer chain [13, 14].

**Table 1.1** Chemical structures of some of the most common conjugated polymers [1, 12].

Name structure	Structure
Polyacetylene	
Polypyrrole	
Polythiophene	
Polyaniline	
Poly(phenylenevinylene)	

The extensive delocalization of the  $\pi$ -electron is well known to be responsible for the array of remarkable characteristic that these polymers tend to exhibit. These characteristic of polymer has been exploited for application in thin film technology field.

### 1.1.1 Conduction mechanisms [15–20]

To explain the mechanism of conductivity in CPs, a band theory has been used as shown in Figure 1.1. According to band theory [15, 16], the electrical properties of direct gap conductive materials are determined by their electronic structures, and the electrons move within discrete energy states called bands. By analogy, the bonding and antibonding  $\pi$ -orbitals of the  $sp^2$  hybridized  $\pi$ -electron materials (e.g. polyenes) generate energy bands, which are fully occupied ( $\pi$ -band) and empty ( $\pi^*$ -band). The highest occupied band is called the valence band, and the lowest unoccupied band is the conduction band. The energy difference between them is called the band gap. Electrons must have certain energy to occupy a given band and need extra energy to move from the valence band to the conduction band. Moreover, the bands should be partially filled in order to be electrically conducting, as neither empty nor full bands can carry electricity.

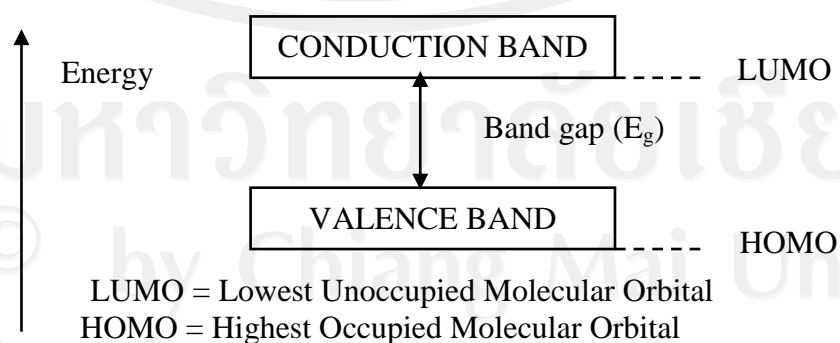


**Figure 1.1** Band structure in an electronically conducting polymer [15, 16].

Electronically conducting polymers are extensively conjugated molecules that they possess a spatially delocalized band-like electronic structure [17]. These bands stem from the splitting of interacting molecular orbitals of the constituent monomer units in a manner reminiscent of the band structure of solid-state semiconductors [18]. It is generally agreed that the mechanism of conductivity in these polymers is based on the motion of charged defects within the conjugated framework. The charge carriers, either positive p-type or negative n-type, are the products of oxidizing or reducing the polymer respectively. The following overview describes these processes in the context of p-type carriers although the concepts are equally applicable to n-type carriers. Oxidation of the polymer initially generates a radical cation with both spin and charge. Borrowing from solid state physics terminology, these species are referred to as a polaron and comprises both the hole site and the structural distortion which accompanies it. The cation and radical form a bound species, since any increase in the distance between them would necessitate the creation of additional higher energy quinoid units. Theoretical treatments have demonstrated that two nearby polarons combine to form the lower energy bipolaron [19, 20]. One bipolaron is more stable than two polarons despite the coulombic repulsion of the two ions. Since the defect is simply a boundary between two moieties of equal energy, the infinite conjugation chain on either side, it can migrate in either direction without affecting the energy of the backbone, provided that there is no significant energy barrier to the process. It is this charge carrier mobility that leads to the high conductivity of these polymers. The conductivity,  $\sigma$  of a conducting polymer is related to the number of charge carriers  $n$  and their mobility. Because the band gap of conjugated polymers is usually fairly large,  $n$  is very small under ambient conditions.

Consequently, conjugated polymers are insulators in their neutral state and no intrinsically conducting organic polymer is known at this time. A polymer can be made conductive by oxidation (p-doping) and/or, less frequently, reduction (n-doping) of the polymer either by chemical or electrochemical means, generating the mobile charge carriers described earlier.

### 1.1.2 Synthesis of conducting polymers [1, 21]

There are numerous synthetic techniques used in the synthesis of conducting polymers. CPs can be synthesized either chemically or electrochemically, with each having advantages and disadvantages as summarized in Table 1.2 [1]. Since most conjugated polymer cannot be dissolved or melted, they must be synthesized directly in desired shape and location. This necessity has frustrated many researchers since the form; most importantly the morphology of the conjugated polymer has one of the greatest influences on many of the properties, most notably the electrical conductivity of the doped polymer. Theory and experiment have placed much emphasis on justifying the formation of mobile, delocalized carriers within the polymer chains (polarons, bipolarons, solitons) [1, 21]. However, since no one polymer strand is long enough to persist over a macroscopic length, the measured conductivity of a polymer sample requires that carriers hop between polymer strands. This hopping is widely believed to limit the bulk conductivity. Synthesis of highly conductive polymer samples has become an art in some circles since small changes in synthesis, catalyst removal, or doping can dramatically affect sample morphology and result in wide variation in conductivity.

**Table 1.2** Comparison of chemical and electrochemical CPs polymerization [1].

<b>Polymerization approach</b>	<b>Advantages</b>	<b>Disadvantages</b>
Chemical polymerization	<ul style="list-style-type: none"> <li>• Larger-scale production possible</li> <li>• Post-covalent modification of bulk CP possible</li> <li>• More options to modify CP backbone covalently</li> </ul>	<ul style="list-style-type: none"> <li>• Cannot make thin films</li> <li>• Synthesis more complicated</li> </ul>
Electrochemical polymerization	<ul style="list-style-type: none"> <li>• Thin film synthesis possible</li> <li>• Ease of synthesis</li> <li>• Entrapment of molecules in CP</li> <li>• Doping is simultaneous</li> </ul>	<ul style="list-style-type: none"> <li>• Difficult to remove film from electrode surface</li> <li>• Post-covalent modification of bulk CP is difficult</li> </ul>

### 1.1.3 Step-growth polymerization [21]

Probably the most common method of chemical synthesis of conjugated polymer is via a step-growth polymerization. Before the advent of the continuous electrochemical synthesis, this method was the only way to make a large amount of polymers such as polythiophene. These polymerizations require a high-yield reaction to proceed to a high degree of polymerization. However, in principle, any monomer that can be oxidatively polymerized electrochemically can be polymerized using a chemical oxidant (e.g.  $\text{FeCl}_3$ ) as well. If the resulting polymer is insoluble, the end of

the polymerization may occur in the solid state. This serious limitation is avoided in the synthesis of soluble conjugated polymers. The example of this type of polymerization is the synthesis of polythiophene and its derivatives. The most commonly performed using a nickel catalyzed couplings, a polymerization based on Friedel-Crafts alkylation, coupling of the di-halide using a Ni(0) catalyst, and direct oxidation with  $\text{FeCl}_3$  are employed as well [21].

#### 1.1.4 Chain-growth polymerizations [21]

Chain-growth polymerizations are useful in the synthesis of conjugated polymers because polymer properties can often be tailored by the selection of catalyst system and because higher molecular weight polymers can be synthesized at a lower degree of conversion of monomer, a point which is particularly attractive when it is necessary to form an insoluble polymer [21]. It has already been pointed out that several conjugated “polymer” are suspected to be oligomers, particularly oxidatively coupled polyparaphenylene, and it is frustrating when the validity of a study must be questioned because it is unclear whether the material under study is really polymeric in nature. Although many would argue that molecular weight has little to do with polymer properties, this promise has little or no experimental verification. Moreover, some of these conjugated polymers are attracting interest as high strength materials, and polymer strength is certainly dependent upon molecular weight.

#### 1.1.5 Ring-opening metathesis polymerization [19, 21]

Ring-opening polymerization can follow either a step-growth or chain growth mechanism and involves the breaking of bond in a ring to form an open-chain intermediate (Figure 1.2). Ring-opening metathesis polymerization (ROMP) involves

the use of a transition metal carbene complex to cut open a cyclic olefin molecule and “stitch” these molecules back together into a polymer chain [19]. This polymerization is of great interest for the synthesis of conjugated polymers because, among other factors, the number of double bonds in the monomer is preserved in the polymer, and because, in principle one can take the repeat unit for any conjugated polymer containing an olefin and cyclize it to form a potential new monomer. Synthetic scheme for ring-opening metathesis polymerization was reported [19]. This polymerization has been very successfully used to form several precursor polymers. However, ROMP has been applied to direct synthesis of conjugated polymers as well.



**Figure 1.2** General schemes for a ring-opening polymerization [19].

### 1.1.6 Electrochemical synthesis [19, 22]

Most conjugated polymers are synthesized by electrochemical means. Pyrrole, thiophene and their derivatives are often polymerized in this manner as are carbazoles, azulenes and pyrenes. Typically, this oxidation is accomplished by placing in the monomer and electrolyte in a suitable solvent such as acetonitrile and oxidizing at a mild potential. A polymer film grows at the anode in a reaction. In principle, any trace species that can react with the propagating radical cation can terminate one end of the polymer. Any polymer chain that does not re-oxidize is effectively terminated as well. The kinetics of this polymerization was expected to be complex. Among other factors, the reaction occurs in a heterogeneous environment, and the polymerization is based upon coupling of the radical cations which can occur

between the oxidized forms of any combination of monomers and polymer chains. New polymers synthesized by this procedure continue to be reported as new oxidizable conjugated units become available [19]. The monomer is electrochemically oxidized at a polymerization potential giving rise to free radicals. These radicals are adsorbed onto the electrode surface and undergo subsequently a wide variety of reactions leading to the polymer network. The electropolymerization should preferably occur in aqueous solution with a neutral pH in order to be incorporated into the polymer film in a suitable form. The growth of this polymer depends on its electrical character. If the polymer is electrically non-conducting, its growth is self-limited. Such films are very thin (10–100 nm). In contrast, the growth of conductive polymers is virtually unlimited. The process is governed by the electrode potential and by the reaction time, which allowing controlling the thickness of the resulting film. The polymerization occurs locally and strictly on the electrode surface. This is particularly suitable for the coating of microelectrodes and microelectrode arrays. In addition, the combination of different conducting or non-conducting polymers allows the building of multilayer structures with extremely low thickness leading to fast responding sensors with reduced interferences. The film can be generated by cycling the potential (potentiodynamically) or at a fixed potential (potentiostatically). Polypyrrole was used for the immobilization of a wide number of enzymes, mainly onto the Pt electrode. The mechanism of the polymerization process, occurring at potentials above +600 mV, is shown in Figure 1.3. The morphology of the film depends on the nature of the electrolyte, the crystallographic structure of the underlying electrode, the speed and the potential of the deposition, the presence of

anions and polyanions or surfactants, the concentration of the monomer, and the pH of the solution.

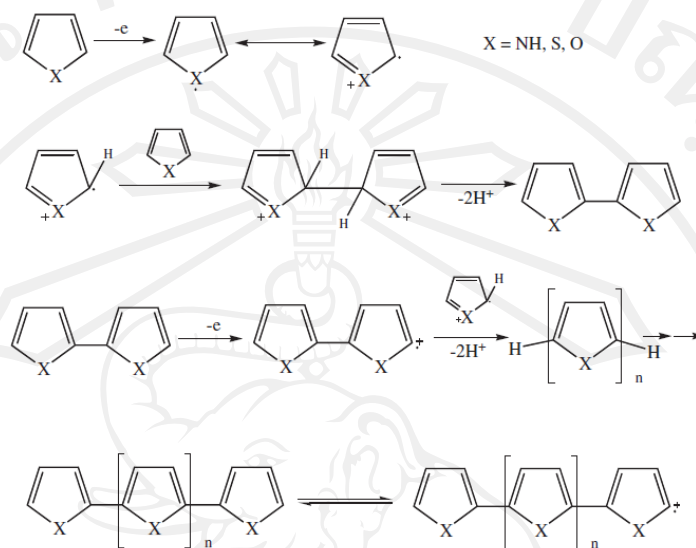


**Figure 1.3** Mechanism for heterocycle polymerization via electrochemical synthesis. X= NH, S, or O. This pathway is initiated by the oxidation of a monomer at the working electrode to give a cation species, which can react with a neutral monomer species or radical cation oligomeric species to generate the polymer [22].

#### 1.1.7 Polyaniline [23–28]

The primary structure of polyaniline (PANI) consists of benzenoid rings with an imine ( $sp^2$  hybridized state) and quinoid rings with an amine ( $sp^3$  hybridized state) as shown in Figure 1.4.

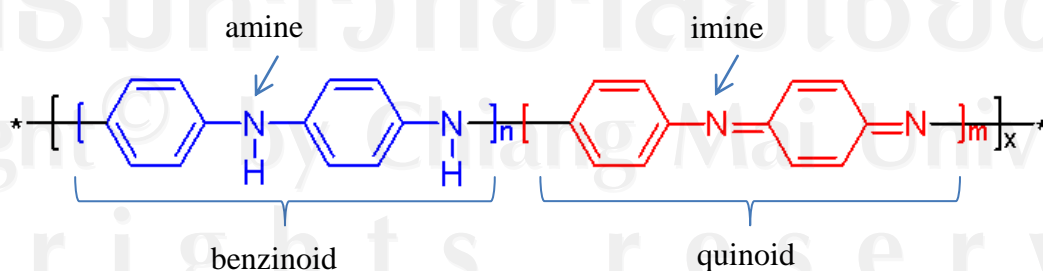


**Figure 1.4** Main PANI structure  $n + m = 1$ ,  $x$  = degree of polymerization [23].

Polyaniline (PANI) is one of CPs has been known and studied extensively since the 1980s [23]. PANI and their derivatives has received considerable attention due to the electrochemical and optical properties with its many attractive properties such as specific binding site, low cost, easily synthesized, environmental stability and potential application in biosensor [24]. The properties of PANI film depend on the oxidation and the protonation state of the film. PANI film was deprotonation and loss in electroactivity at pH higher than 4 [9]. PANI has three main stable oxidation states range from fully reduce leucoemeraldine ( $n = 1, m = 0$ ) is found to be insulating and yellow color. The half-oxidized is called emeraldine ( $n = m = 0.5$ ). The most common green protonate emeraldine salt has conductivity on a semiconductor and convert to a non-conducting blue emeraldine base when treated with ammonium hydroxide solution [25] as shown in Figure 1.5.

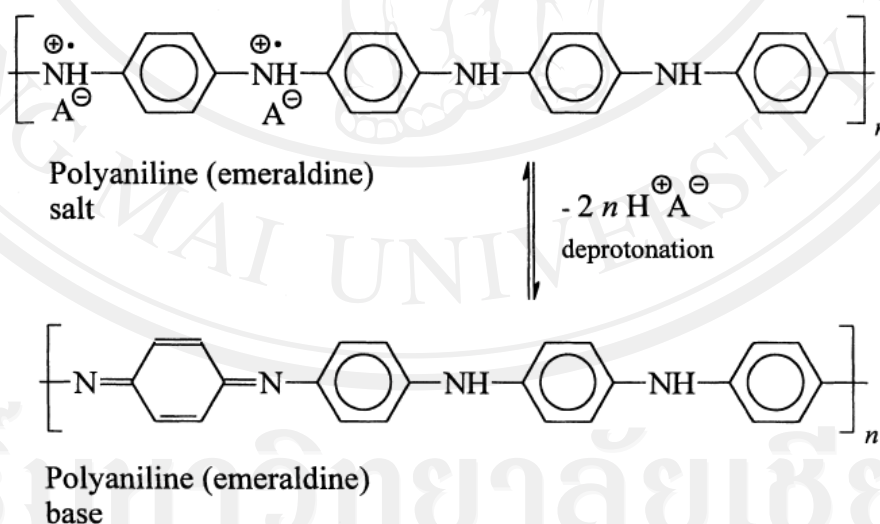


**Figure 1.5** PANI (emeraldine) salt in the alkaline medium convert to PANI (emeraldine) base.  $\text{A}^-$  is an alkali ion [25].

The fully oxidized pernigraniline ( $n = 0$ ,  $m = 1$ ) is insulating and violet color. The color change of each three oxidation state of PANI can be used in sensor and electrochromic devices [26]. The doping in polymer to conductive form is an oxidation (p-type doping, withdraw electron from polymer chain) or reduction (n-type doping, add electron into polymer chain) process, rather than atom replacement in inorganic semiconductors. In the case of PANI oxidation, the halogen molecule attracts an electron from the PANI and PANI become positive charged. The CPs does not have only  $\pi$ -conjugated chain but also containing counter-ions caused by doping. The insulating  $\pi$ -conjugated polymers can be converted to conducting polymers by a chemical or electrochemical doping and which can be consequently returned to insulate state by de-doping. This suggests that not only de-doping can take place in CPs, but also reversible doping/de-doping process, which is different from inorganic semiconductor where de-doping can't take place [27]. The electronic properties of PANI and their derivatives were opened a large window for the biosensor applications.

Conducting polymers (CPs) have numerous (bio)analytical and technological applications. CPs are easily synthesized and deposited onto the conductive surface of a given substrate from monomer solutions by electrochemical polymerization with precise electrochemical control of their formation rate and thickness. Coating electrodes with CPs under mild conditions opens up enormous possibilities for the immobilization of biomolecules and bioaffinity or biorecognizing reagents, improve their electrocatalytic properties, rapid electron transfer and direct communication to produce a range of analytical signals and new analytical applications [1, 28–30].

### 1.1.8 Electrochemical set up [31–34]

An electrochemical cell must consist of at least two electrodes and one electrolyte. An electrode may be considered to be an interface at which the mechanism of charge transfer changes between electronic (movement of electrons) and ionic movement of ions. An electrolyte is a medium through which charge transfer can take place by the movement of ions. An electrochemical cell containing a working electrode, a counter electrode, and a reference electrode is shown in Figure 1.6. In all electrochemical experiments, the reactions of interest occur at the surface of the working electrode. Therefore, in controlling the potential drop across the interface between the surface of the working electrode and the solution (i.e., the interfacial potential) is the prime interest. However, it is impossible to control or measure this interfacial potential without placing another electrode in the solution. Thus, two interfacial potentials must be considered, neither of which can be measured independently. Hence, one requirement for this counter electrode is that its interfacial potential remains constant, so that any changes in the cell potential produce identical changes in the working electrode interfacial potential. An electrode whose potential does not vary with current is referred to an ideal non-polarizable electrode, and is characterized by a vertical region on a current vs potential plot. However, there is no electrode that behaves in this way (although some approach ideal non-polarizable behavior at low currents). Consequently, the interfacial potential of the counter electrode in the two-electrode system discussed above varies as current is passed through the cell. This problem is overcome by using a three-electrode system, in which the functions of the counter electrode are divided between the reference and auxiliary electrodes; that is, the potential between the working and reference

electrodes is controlled and the current passes between the working and auxiliary electrodes. The current passing through the reference electrode is further diminished by using a high-input-impedance operational amplifier for the reference electrode input. A current may flow between the working and counter electrodes, while the potential of the working electrode is measured against the reference electrode. This setup can be used in basic research to investigate the kinetics and mechanism of the electrode reaction occurring on the working electrode surface, or in electroanalytical applications.

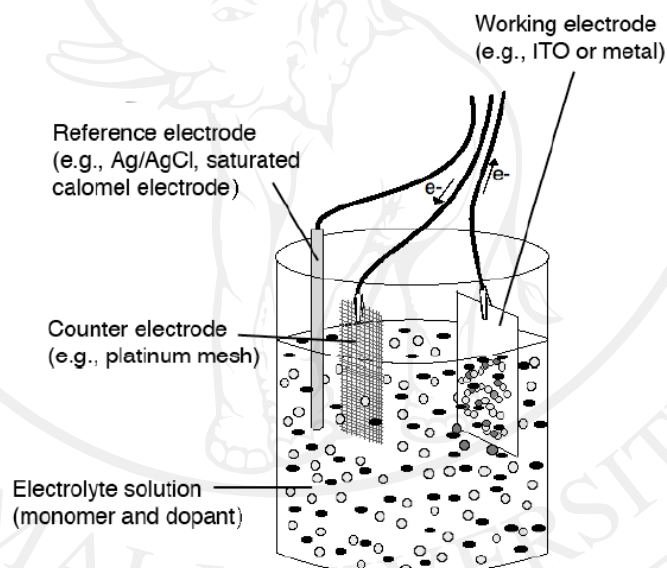


**Figure 1.6** Electropolymerization setup[22].

#### 1.1.8.1 Working electrodes or indicator electrodes [32–34]

This is the electrode at which the electrochemical phenomena being investigated takes place. There are a number of noble metal electrodes currently available for voltammetric studies. The frequently use electrodes are platinum, gold and silver followed occasionally by palladium, rhodium and iridium. Various polycrystalline forms including sheets, rods and wires are commercially available in high purity and

the materials are readily machined into useful shapes. All of the noble metals have an over potential for hydrogen evolution. The noble metal electrodes adsorb hydrogen on their surfaces although gold does so to a lesser extent. Palladium adsorbs hydrogen into the bulk metal in appreciable quantities and is not recommended for use as a cathode in protic solvents. As an inert electrode material, carbon is useful for both oxidation and reduction reaction either aqueous or non-aqueous solutions. Only graphitic forms of carbon are therefore useful as electrode materials. Ordinary spectroscopic grade of graphite rods can be used for work in which the surface area of the electrode does not need to be well defined. Other types of carbon electrode include the glassy carbon electrode and the carbon paste electrode.

#### 1.1.8.2 Counter or auxiliary electrode [32–34]

This electrode which serves as a source or sink for electrons so that current can be passed from the external circuit through the cell. In general, neither its true potential nor current is ever measured or known. That is used only to make an electrical connection to the electrolyte so that a current can be applied to the working electrode. The processes occurring on the counter electrode are not important; it is usually made of inert materials (noble metals or carbon/graphite) to avoid its dissolution. This is the case for cells used for research or for electroanalytical purposes. Of course, for many practically used cells, the processes occurring on both electrodes can be very important and also called “auxiliary” electrode.

#### 1.1.8.3 Reference electrodes [32–34]

This is the electrode whose potential is constant enough that it can be taken as the reference standard against the potentials of the other electrodes present in the cell can

be determined. The ideal reference electrode should possess the following properties:

- it should be reversible and obey the Nernst equation with respect to some species in the electrolyte
- its potential should be stable with time
- its potential should return to the equilibrium potential after small currents are passed through the electrode
- if it is an electrode like the Ag/AgCl reference electrode, the solid phase must not be appreciably soluble in the electrolyte
- it should show low hysteresis with temperature cycling

#### 1.1.8.4 Silver/silver chloride reference electrode [32–34]

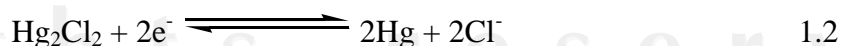
The redox process for this electrode is



This electrode consists of a silver wire, coated with silver chloride, which is immersed in a solution containing chloride ions. This electrode uses an aqueous solution containing 3 M sodium chloride; a porous frit is used for the junction between the reference electrode solution and the sample solution. The potential  $E$  for any electrode is determined by the Nernst equation, which relates  $E$  to the standard potential  $E^0$  and the activities of the redox components (the standard potential is the potential of the electrode at unit activity under standard conditions).

#### 1.1.8.5 Saturated calomel reference electrode [32–34]

The redox process for this electrode is



The saturated calomel electrode (SCE) is an H-cell. One arm contains mercury covered by a layer of mercury (II) chloride (calomel). This is in contact with a saturated solution of potassium chloride; a porous frit is again used for the junction between the reference electrode solution and the sample solution at the end of the other arm. Once assembled, the electrode should be stored with porous frit and immersed in a saturated solution of potassium chloride to maintain the chloride concentration in the reference electrode.

#### 1.1.8.6 Pseudo-reference electrode [32–34]

Pseudo-reference electrodes are simply metal wires (e.g., platinum or silver) immersed in the sample solution. Although such electrodes do provide a constant potential, the reference potential is unknown, and is dependent on the composition of the sample solution. Consequently, redox potentials measured using a pseudo-reference electrode should be quoted relative to redox potential of the internal reference compound. One advantage of pseudo-reference electrodes is its low impedance.

#### 1.1.8.7 Silver/silver ion electrode

The redox process for this electrode is



This electrode is less stable than the aqueous electrodes discussed above (due to diffusion of silver ions out of the electrode and the photo reactivity of these ions), and must be prepared frequently. Bioanalytical System, Inc. (BASi) provides a non-aqueous reference electrode kit, which requires assembly by the user. The BASi non-aqueous reference electrode consists of a silver wire immersed in a solution of silver

nitrate or perchlorate (0.001 M to 0.01 M) and electrolyte (e.g., 0.1 M tetrabutylammonium perchlorate, (TBAP) in the desired organic solvent. Suitable organic solvents include acetonitrile, dimethylsulfoxide, methanol, ethanol and tetrahydrofuran. Silver ions are reduced by dimethylformamide and are insoluble in methylene chloride; these solvents are therefore not suitable for this reference electrode (acetonitrile can be used as the reference electrode solvent when one of these other two solvents is used for the sample solution). The potential for the silver/silver ion reference electrode depends on the solvent, the silver ion concentration the nature and concentration of the electrolyte. It is also changed by the introduction of salt bridges, which are used to decrease the contamination of the sample solution by the effect of silver ions.

#### 1.1.8.8 Electrolyte solutions [31, 32]

The medium is required for electrochemical experiment is electrolyte solutions which must be able to conduct the current. This can be achieved by using either a molten salt or an electrolyte solution. An electrolyte solution is made by adding an ionic salt to an appropriate solvent. The salt must be fully dissociated in the solvent in order to generate a conducting (i.e., ionic) solution. The electrolyte solution must also be able to dissolve the analyte, an electrochemically inert over a wide potential range (i.e., no current due to electrolyte solution oxidation/reduction), and must be pure (e.g., the presence of water decreases the size of the potential range). It is chemically inert, so that it will not react with any reactive species generated in the experiment (e.g., acetonitrile is nucleophilic, which can react with electrogenerated cations). If the temperature is to be varied, the electrolyte solution must have an appropriate solubility range. Electrolyte solutions can be aqueous or non-aqueous. A wide range

of salts can be used for aqueous electrolyte solutions. Since the redox potentials of some compounds are pH sensitive, buffered solutions should be used for these compounds. Suitable non-aqueous solvents include acetonitrile, dimethylformamide, dimethyl sulfoxide, tetrahydrofuran, methylene chloride, and propylene carbonate. Salts for non-aqueous electrolyte solutions typically consist of a large cation (e.g., tetra-alkylammonium cations), and large anions (e.g., hexafluorophosphate, tetrafluoroborate, and perchlorate) to ensure a full dissociation. Perchlorate salts should be handled with care, since they are potentially explosive.

### 1.2 Cyclic voltammetry (CV) [35–38]

Cyclic voltammetry (CV) is an electrolytic method that uses microelectrodes and an unstirred solution so that the measured current is limited by analyte diffusion at the electrode surface. The electrode potential is ramped linearly to a more negative potential, and then ramped in reverse back to the starting voltage. The forward scan produces a current peak for any analyses that can be reduced through the range of the potential scan. The current will increase as the potential reaches the reduction potential of the analyte, but then falls off as the concentration of the analyte is depleted close to the electrode surface. As the applied potential is reversed, it will reach a potential that will re-oxidize the product formed in the first reduction reaction, and produce a current of reverse polarity from the forward scan. This oxidation peak will usually have a similar shape to the reduction peak. The peak current,  $i_p$ , is described by the Randles-Sevcik equation:

$$i_p = (2.69 \times 10^5) n^{3/2} A C D^{1/2} v^{1/2} \quad 1.4$$

where  $n$  is the number of moles of electrons transferred in the reaction

$A$  is the surface area of the electrode

C is the analyte concentration (in mole/cm<sup>3</sup>)

D is the diffusion coefficient

v is the scan rate of the applied potential

The potential difference between the reduction and oxidation peaks is theoretically 59 mV for a reversible reaction. In practice, the difference is typically 70–100 mV. Larger differences, or non-symmetric reduction and oxidation peaks are an indication of a nonreversible reaction.

### 1.2.1 Cyclic voltammetry primer [35, 36]

A simple potential wave form that is often used in electrochemical experiment is the linear wave form i.e., the potential is continuously changed as a linear function of time. The rate of change of potential with time is referred to as the scan rate (v). The simplest technique that uses this wave form is linear sweep voltammetry. The potential range is scanned in one direction, starting at the initial potential and finishing at the final potential. A more commonly used variation of the technique is cyclic voltammetry, in which the direction of the potential is reversed at the end of the first scan. Thus, the waveform is usually of the form of an isosceles triangle. This has the advantage that the product of the electron transfer reaction that occurred in the forward scan can be probed again in the reverse scan. In addition, it is a powerful tool for the determination of formal redox potentials, detection of chemical reactions that precede or follow the electrochemical reaction and evaluation of electron transfer kinetics [35]. In this example it is assumed that only the reduced form of the species is initially present. Thus, a positive potential scan is chosen for the first half cycle during which an anodic current is observed. The reason by, the solution is quiescent; the product generated during the forward scan is available at the surface of the electrode

for the reverse scan resulting in a cathodic current. Complex wave form composed of two isosceles triangles. The voltage is first held at the initial potential where no electrolysis occurs and hence no faradaic current flows. As the voltage is scanned in the positive direction, so the reduced compound is oxidized at the electrode surface. At a particular set value, the scan direction is reversed and the material that was oxidized in the outward excursion is then reduced. Once the voltage is returned to the initial value, the experiment can be terminated. In this example however a further voltage excursion takes place to more negative (more reducing) values. This may be useful in probing for other species present in the sample or for investigating any electroactive products formed as a result of the first voltage excursion. The situation is very different when the redox reaction is not reversible, when chemical reactions are coupled to the redox process or when adsorption of either reactants or products occurs. In fact, it is these "non-ideal" situations which are usually of greatest chemical interest and for which the diagnostic properties of cyclic voltammetry are particularly suited. An example wave form that can be used in cyclic voltammetry is shown in Figure 1.7.

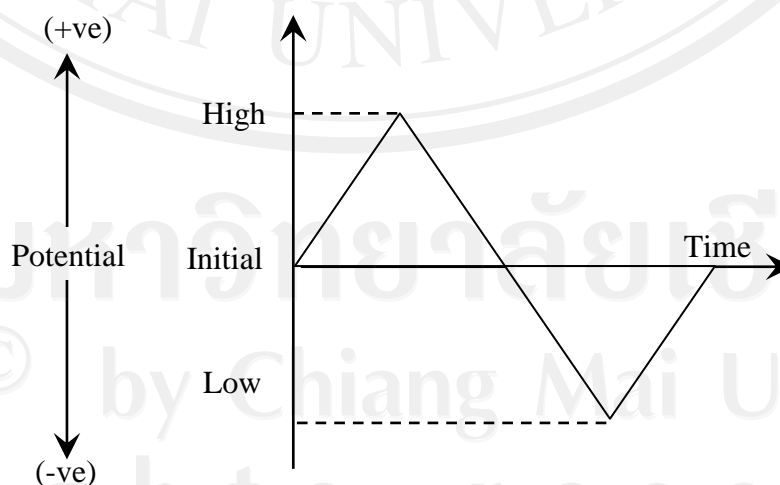


**Figure 1.7** Normal wave form of cyclic voltammetry [35].

The basic shape of the current response for a cyclic voltammetry experiment is shown in Figure 1.8 [36]. At the start of the experiment, the bulk solution contains only the reduced form (R) of the redox couple (I) so that at potentials lower than the redox potential, i.e. the initial potential, there is no net conversion of R into the oxidized form (O) at point A. As the redox potential is approached, there is a net anodic current which increases exponentially with potential. As R is converted into O, concentration gradients are set up for both R and O, and diffusion occurs down these concentration gradients. At the anodic peak (point B), the redox potential is sufficiently positive that any R that reaches the electrode surface is instantaneously oxidized to O. Therefore, the current now depends upon the rate of mass transfer to the electrode surface and so the time dependence is quartet resulting in an asymmetric peak shape.

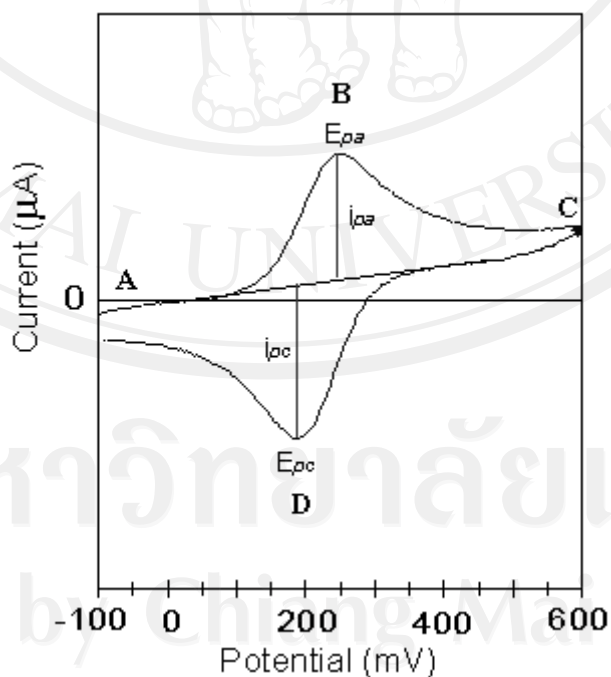


**Figure 1.8** The basic shape of the current response for a cyclic voltammetry [36].

Upon reversal of the scan (point C), the current continues to decay with a quartet until the potential nears the redox potential. At this point, a net reduction of O to R occurs which causes a cathodic current which eventually produces a peak shaped response (point D).

The situation is very different when the redox reaction is not reversible, when chemical reactions are coupled to the redox process or when adsorption of either reactants or products occurs. In fact, it is these "non-ideal" situations which are usually of greatest chemical interest and for which the diagnostic properties of cyclic voltammetry are particularly suited.

### 1.2.2 Mechanistic complications [35, 36]

#### 1.2.2.1 Nernstian (reversible) behavior

If a redox system remains in equilibrium throughout the potential scan, the electrochemical reaction is said to be reversible. In other words, equilibrium requires that the surface concentrations of oxidation and reduction are maintained at the values required by the Nernst Equation. Under these conditions, the following parameters characterize the cyclic voltammogram of the redox process.

- The peak potential separation ( $E_{pa} - E_{pc}$ ) is equal to  $57/n$  mV for all scan rates where  $n$  is the number of electron equivalents transferred during the redox process.
- The peak width is equal to  $28.5/n$  mV for all scan rates.
- The peak current ratio ( $i_{pa}/i_{pc}$ ) is equal to 1 for all scan rates.
- The peak current function increases linearly as a function of the square root of  $v$ .

The system under investigation is a simple one electron reversible couple so under the conditions of the experiment, the above parameters are observed. Cyclic

voltammograms for ferrocene carboxylic acid in an aqueous pH 7.0 phosphate buffer electrolyte as shown in Figure 1.9.

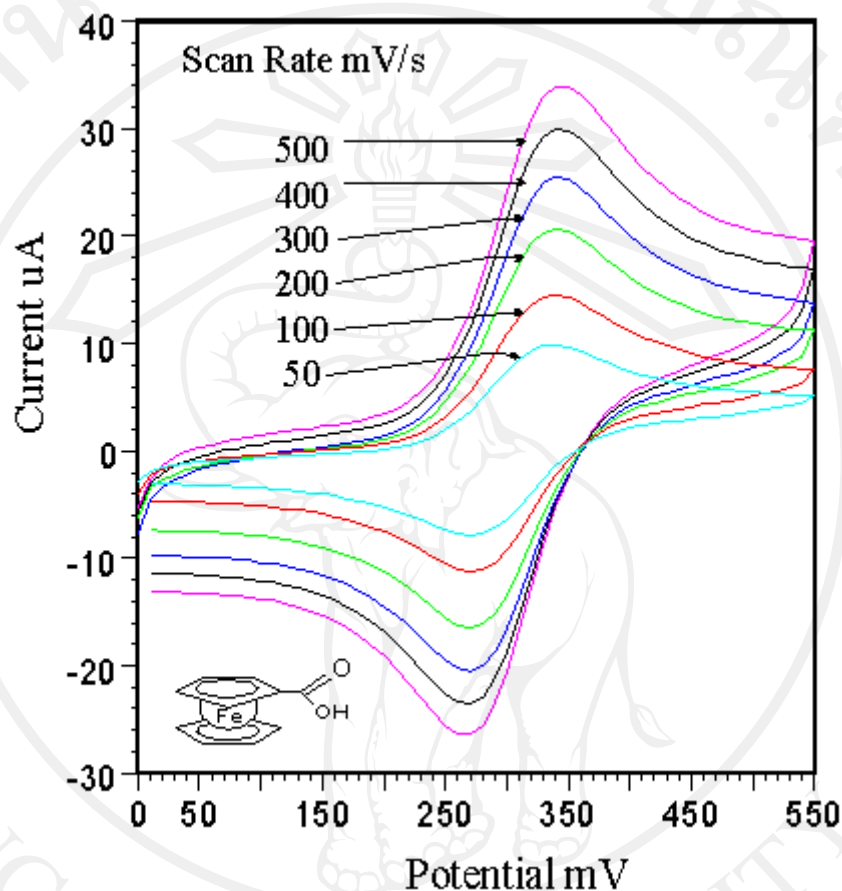


**Figure 1.9** Cyclic voltammograms for ferrocene carboxylic acid at different scan rate [36].

As the voltage becomes increasingly more positive (oxidizing) value is reached where ferrocene carboxylic acid (reduced form) is converted to the oxidized ferricinium species. This results in the appearance of the anodic peak. Assuming that the reaction kinetics are very fast compared to the scan rate, the equilibrium involving the concentrations of reduced and oxidized species at the electrode surface will adjust rapidly according to the Nernst equation;

$$E = E^{o'} + (RT/nF) \ln C_O / C_R \quad 1.5$$

where  $C_O$  and  $C_R$  represent the surface concentration of oxidized and reduced species, respectively. If the system is diffusion controlled (the normal situation for cyclic voltammetry) then Fick's law of diffusion holds for both O and R. Under these conditions, the peak current ( $i_p$ ) is followed by the Randles-Sevcik equation:

$$i_p = 2.69 \times 10^5 n^{3/2} A D_O^{1/2} v^{1/2} C_O \quad 1.6$$

where  $A$  is the electrode area ( $\text{cm}^2$ ),  $n$  is the number of electrons transferred,  $D_O$  is the diffusion coefficient,  $C_O$  is the concentration ( $\text{mol}\cdot\text{cm}^{-3}$ ) and  $v$  is the scan rate (volt/s).

The basic shape of cyclic voltammograms of EC mechanism with different first-order rate constant ( $k_f$ ) and heterogeneous electron transfer rate ( $k_{\text{het}}$ ) are shown in

Figure 1.10.

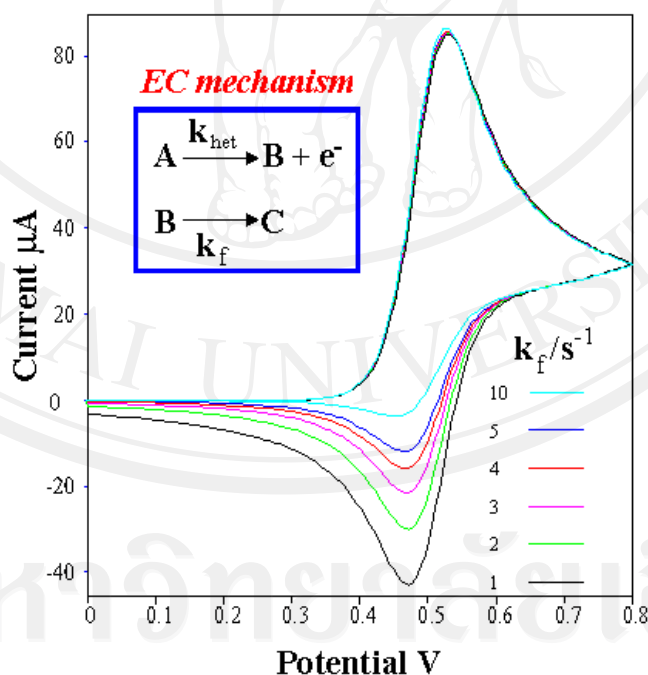


**Figure 1.10** The basic shape of cyclic voltammograms of EC mechanism with different first-order rate constant ( $k_f$ ) [36].

### 1.2.2.2 The Electrochemical Chemical (EC) mechanism [35, 36]

The shape of a voltammogram can be significantly altered if there is a coupled chemical reaction either before or after occurred in the electrochemical process. Further complications attributed to the chemical nature of the reaction, the degree of reversibility, the rate and equilibrium constants of the process can all play a part in the final shape of the voltammogram and on the information that can be obtained from a set of experiments. In general terms, coupled mechanistic schemes are described by the letters E (electrochemical) and C (chemical). The order in which they are written denotes the order in which the processes occur. Thus an EC mechanism describes a process in which an electrochemical step is followed by a chemical step which is then followed by an electrochemical step. A chemical step is a step where no electron-transfer to or from the electrode takes place. Such a step does not by itself produce a charge flow into or out of the electrode and thus is not directly observable by an external measuring circuit. It may however influence charge flow because of other steps in the mechanism which can be detected indirectly. The chemical step is not directly influenced by the electrode potential. An electrochemical step on the other hand involves electron flow to and from the electrode and as such produces a flow of charge that can be monitored by the external measuring circuit is shown in Figure 1.11.

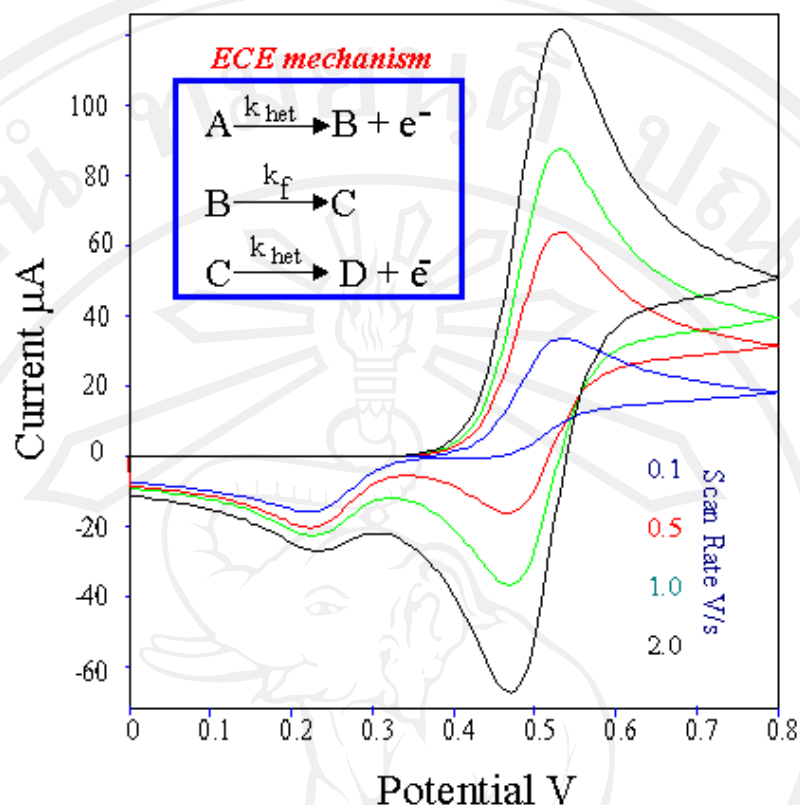


**Figure 1.11** The basic shape of cyclic voltammograms of EC mechanism with different scan rates [36].

### 1.2.2.3 Dealing with an EC mechanism [36]

The following experimental parameters were used to obtain the simulated voltammograms shown; electrode area =  $0.1 \text{ cm}^2$ ,  $k_{\text{het}} = 1 \text{ cm s}^{-1}$ ,  $\nu = 1 \text{ volt s}^{-1}$ ,  $E^0 = 0.5 \text{ V}$  and  $D_O = D_R = 1 \times 10^{-5} \text{ cm}^2 \text{ s}^{-1}$ . Consider the following generalized mechanistic scheme, this shows a typical EC mechanism. In the first step (E), a reduced species is oxidized at the surface of an electrode. The product of the reaction O is unstable and once formed, reacts chemically (C) for example with itself, neighboring molecules or with the solvent to give a new species A which is either electro-inactive or simply not electroactive within the potential window of interest. An example of this type of mechanism is the electrochemical oxidation of ascorbic acid (vitamin C) and its

subsequent reaction with water (the solvent) to yield electrochemically inactive dehydroascorbic acid. The electrochemical reaction is characterized by the heterogeneous rate constant  $k_{\text{het}}$  which we can assume to be very fast. The chemical reaction is characterized by a homogeneous first order rate constant  $k_f$  for which the equilibrium constant  $K$  is equal to;

$$K = [A]_o / [O]_o \quad 1.7$$

where the concentrations of A and O are surface concentrations. The resultant voltammograms for such a process would be similar to those depicted above. Close inspection of the diagram reveals that the forward scan (the oxidation of R to O) is unaffected but the reverse scan (O to R) is altered. An important parameter in determining the shape of the voltammogram is the dimensionless ratio  $k_f/s^{-1}$ . Because the homogeneous step has a finite rate constant associated with it, there will be a limiting sweep rate ( $s^{-1}$ ) which is fast enough to have completed the reverse scan before any conversion of O to A has taken place. Under these conditions, the voltammogram will not be altered in any way and the ratio of the two peak currents will be unity. This feature can be best understood by looking at the simulated voltammograms. In this case, the voltammograms for an EC reaction are recorded at increasing scan rates (1 to 10  $\text{Vs}^{-1}$ ). It is evident, that as the scan rate is increased, the contribution from the homogeneous reaction becomes less pronounced and the voltammogram approaches the shape of that for a normal, uncomplicated situation. The following experimental parameters were used to obtain the simulated voltammograms shown; electrode area =  $0.1 \text{ cm}^2$ ,  $k_{\text{het}} = 1 \text{ cm s}^{-1}$ ,  $E^0 = 0.5 \text{ V}$ ,  $D_O = D_R$

$= 1 \times 10^{-5} \text{ cm s}^{-1}$  and  $k_f = 10 \text{ s}^{-1}$ . The basic shape of cyclic voltammograms of EC mechanism with different scan rates is shown in Figure 1.12.

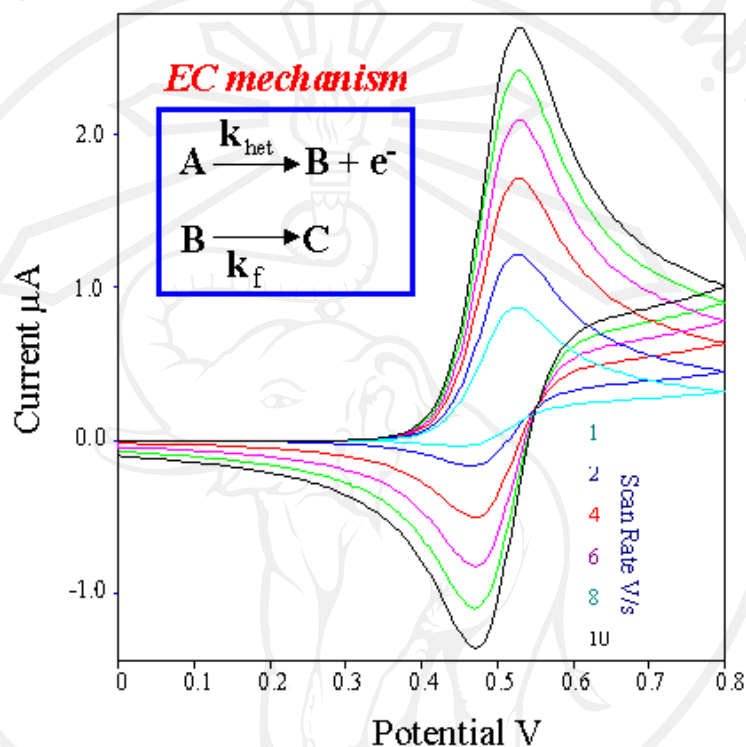


**Figure 1.12** The basic shape of cyclic voltammograms of EC mechanism with different scan rates [36].

### 1.3 Surface Plasmon Resonance Spectroscopy (SPR) [39–41]

#### 1.3.1 Theoretical background

SPR is a technique which associated with the total internal reflection of light (evanescent wave) at the boundary between two media of different optical properties described by their different dielectric function,  $\epsilon_i$  [39]. The example of this observation is the boundary between a glass prism and water. A plane wave from a laser light source (wavelength  $\lambda$ ) or incoming light impinging upon the interface from glass side, i.e. from material with higher refractive index, will be totally (internally)

reflected if the angle of incidence exceeds a critical value,  $\theta_c$ . This can be observed by recording the reflectivity,  $R$  (the ratio between reflected and incoming intensity) with a diode detector as a function of the angle of incidence,  $\theta$ . In typical experiment, at angles of incidence smaller than  $\theta_c$ , most of incoming light is transmitted and therefore the reflectivity is low. When the angle of incidence approaches  $\theta_c$ , the reflectivity reaches unity. The evanescent wave is an electromagnetic field which the electric field perpendicular to the interface ( $E_z$ ) does not fall to zero abruptly but decays exponentially with a decay length,  $l$ . This decay length is a function of the angle of incidence. On the other hand, the component along the propagation direction ( $E_x$ ) had the usual oscillatory character of an electromagnetic mode. The evanescent wave is formed at the angle greater than critical angle. When the interface between a metal and a dielectric material is considered, the term “plasmon surface polaritons (PSP) or surface plasmons” for short was described [39–41]. The coupling of the collective plasma oscillations (called “plasmon”) of the nearly free electron gas in a metal to an electromagnetic field has been shown to produce the surface plasmon. This surface plasmon propagates at the metal/dielectric material with the coupling angle which can be excited with photons when the energy and momentum matching conditions between photons and surface plasmons has reached [39–41].

### 1.3.2 The architecture of experimental setup

Three different coupling schemes had been proposed among which are grating, edge, and prism [40]. The different schemes by using prism have been widely used for many applications. In principle, there are two concepts for this experimental setup: Otto-configuration and Kretschmann configuration. The latter one is the most widely used and convenient configuration because the resulting plasmon can be observed

directly through the metal. In the Otto-configuration, photons are not coupled directly to the metal/dielectric interface, but via the evanescent tail of light totally internally reflected at the base of a high-index prism ( $\epsilon_p > \epsilon_d$ ). By choosing the appropriate angle of incidence, resonant coupling between evanescent photons and surface plasmons can be obtained. This resonant coupling is observed by monitoring the laser light, which is reflected by the base of prism, as a function of the incident angle. However, since the major technical drawback of this configuration is the need to obtain the metal surface close enough to the prism base, typically  $\sim 200$  nm. This means even a few dust particles can be the spacers preventing the efficient coupling. As this drawback, the Otto-configuration has not gained any practical importance despite its potential importance for the optical analysis of polymer coated bulk metal samples. On the other hand, the experimentally easier and hence the most wide spread configuration, Kretschmann configuration, has the similar scheme for exciting surface plasmons to Otto-configuration. In Kretschmann configuration, photons in the prism couple through a very thin metal layer (typically  $\sim 45\text{--}50$  nm thick), which is deposited directly onto the base of the prism or onto a glass slide, to surface plasmons at the other side in contact with the dielectric medium. In qualitative, the same consideration for energy and momentum matching are applied as discussed in Otto configuration. Quantitatively, however, the finite thickness of the metal layer causes some modification of the dispersion behavior at surface plasmons. By solving Maxwell's and/or Fresnel's equations for the layer architecture of glass/Ag-layer/dielectric, the angular dependence of the reflectivity can be described.

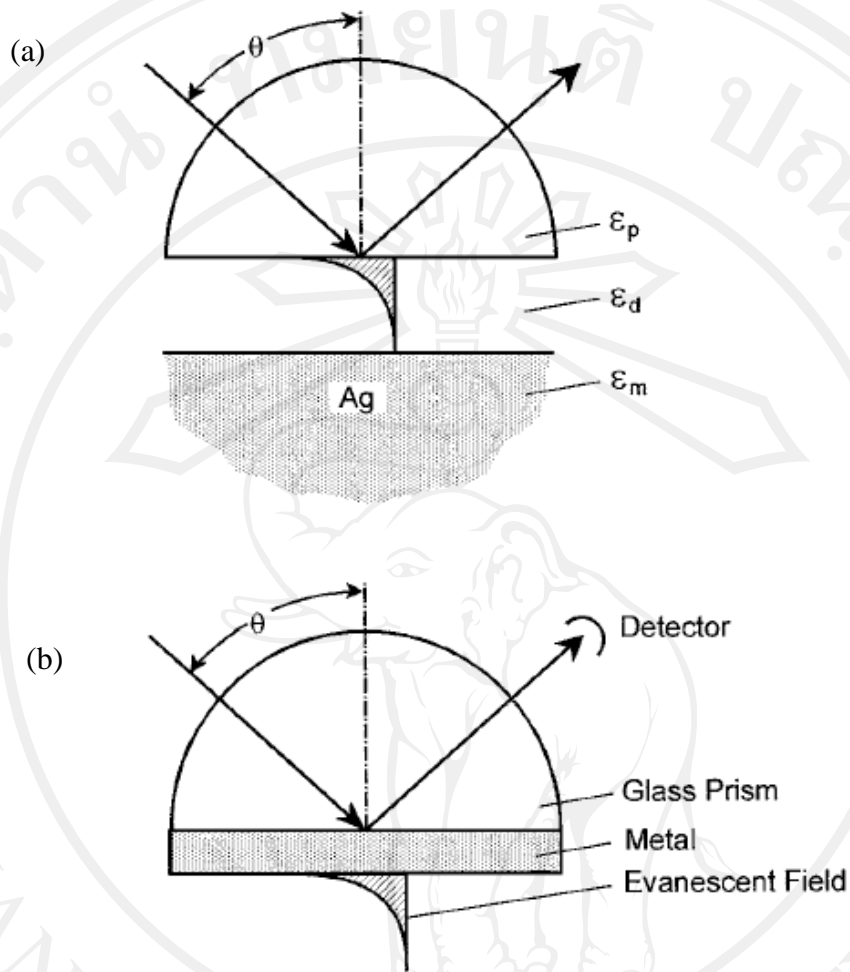


**Figure 1.13** Two concept for experimental setup of surface plasmon resonance spectroscopy (a) The Otto-configuration (b) Kretschman configuration with attenuated total internal reflection (ATR) construction [39].

### 1.3.3 SPR for investigation of the adsorption processes

SPR has been shown to be a technique which has high sensitivity for characterization of ultrathin film, interfaces, and kinetic processes at the nanometer scale [39, 42, 43]. The experimental SPR system for characterization of ultrathin films which relatively simple. A laser beam of wavelength  $\lambda$  incidents at angle  $\theta$  on the noble metal coated base of the prism, which is covered with the thin film of interest

material, is reflected. The intensity of the reflected light is then monitored with a detector as function of  $\theta$ . The curve labeled was taken in air on a bare Au-film evaporated-deposited onto the prism base. The deposition of an ultrathin organic layer of interest molecules which can be prepared by spontaneous self-assembly process, Langmuir-Blodgett (LB) technique, layer by layer deposition method or even simple technique; spin-coating, from solution to Au-surface results in a shift of the curve for PSP running along this modified interface and hence in a shift of the resonance angle (from  $\theta$  to  $\theta^1$ ). The example for using of SPR to in situ investigation of the self-assembly polymer solution adsorption process was studied by Knoll group [42].

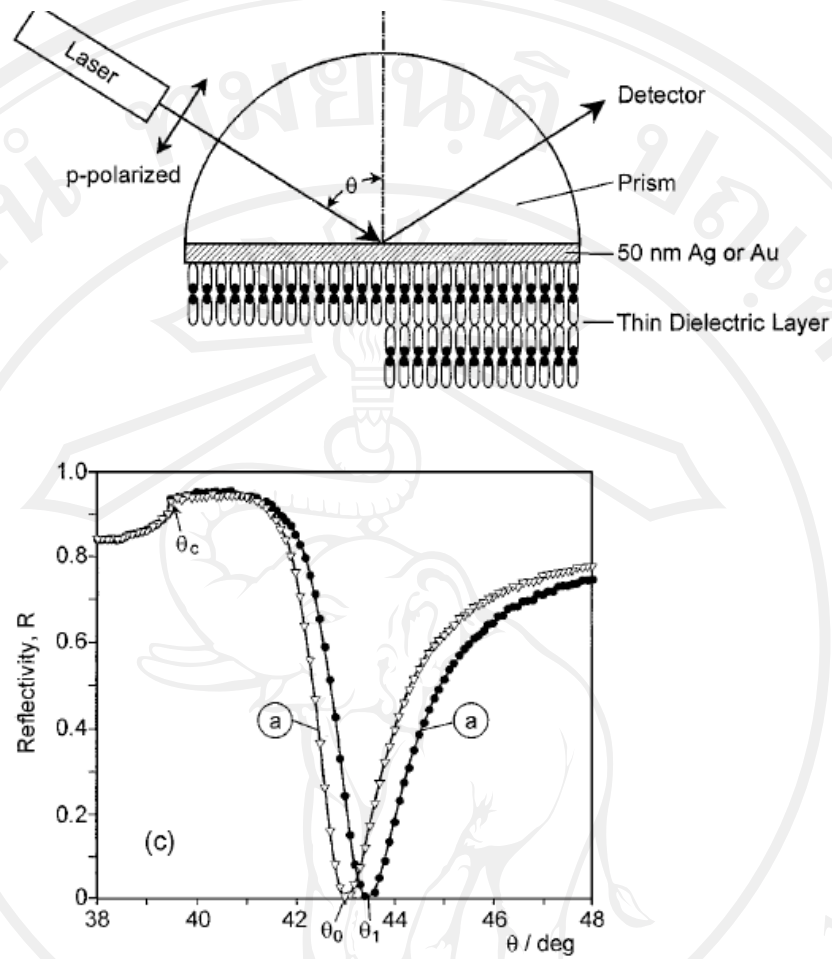


**Figure 1.14** Schematic of the experimental system for SPR reflectivity curve obtained from a bare Au-film and self-assembled monolayer [39].

The experimental setup in this study is Kretschmann configuration with ATR condition. The monolayers of each interest materials were stepwisely deposited by LB process onto the high refractive index glass/Au/octadecyl-thiol layer. A sequence of reflectivity data taken after consecutive depositions showed the linear increases of the multilayer thickness after analysis with Fresnel equation [42]. In addition, the other information, which can be studied by using SPR, is the kinetic information on the interfacial of the multilayer. The kinetic information on any changes of the interfacial

architecture is the time-dependant process which can be obtained by monitoring the reflectivity at a fixed angle of observation,  $\theta^{\text{obs}}$ . At  $t = 0$ , the solution is injected and the adsorption followed in real time as a change in reflectivity. The adsorption process for each layer is complete after several minutes, thus giving the important information for the subsequence of the alternating multilayers preparation.

#### 1.3.4 Electrochemical-Surface Plasmon Resonance Spectroscopy (EC-SPR) [23, 39–44]

The combination of SPR, particularly in the Kretschmann configuration, with electrochemical measurements has become a powerful technique for simultaneous characterization and manipulation of an electrode/electrolyte interfaces [23, 39–43].

This combination has been known as Electrochemical-Surface Plasmon Resonance Spectroscopy (EC-SPR). A schematic diagram for EC-SPR set up is shown in Figure 1.15.

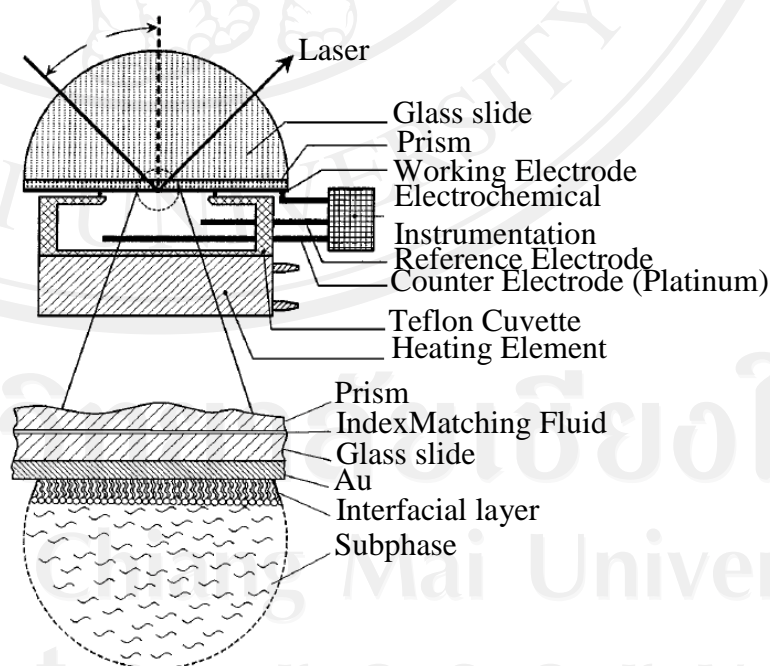


**Figure 1.15** Schematic diagram showing the experimental set up of EC-SPR [39].

The gold substrate which carries the optical surface mode is simultaneously used as the working electrode in electrochemical experiments. One advantage of EC-SPR is that the electrochemical and optical properties can be obtained simultaneously during film forming on the nanometer thickness scale [23, 39]. Recently, EC-SPR was applied for characterization of a number of conducting polymer films including polyaniline [41, 43] and poly(3,4-ethylenedioxythiophene) [42]. The time dependent processes could be induced by a potential sweep which the setup allows simultaneously record the reflectivity and the flow of charges through the electrical circuit, e.g. a classical cyclic voltammogram. In addition, the EC-SPR technique had also been applied to many applications including biosensor development [9, 44].

#### **1.4 Biomolecules (such as catecholamine, uric acid and ascorbic acid) [45–50]**

##### 1.4.1 Catecholamine

A catecholamine (CA) is an organic compound that has a catechol (benzene with two hydroxyl side groups) and a side-chainamine [45] as shown in Figure 1.16. A catechol is a 1,2-dihydroxybenzene group. Catecholamines derive from the amino acid tyrosine [46]. Catecholamines are water-soluble and are 50%–bound to plasma proteins, so they circulate in the blood stream. In the human body, the most abundant catecholamines are epinephrine (adrenaline), norepinephrine (noradrenaline) and dopamine, all of which are produced from phenylalanine and tyrosine. Release of the hormones epinephrine and norepinephrine from the adrenal medulla of the adrenal glands is part of the fight-or-flight response [49].

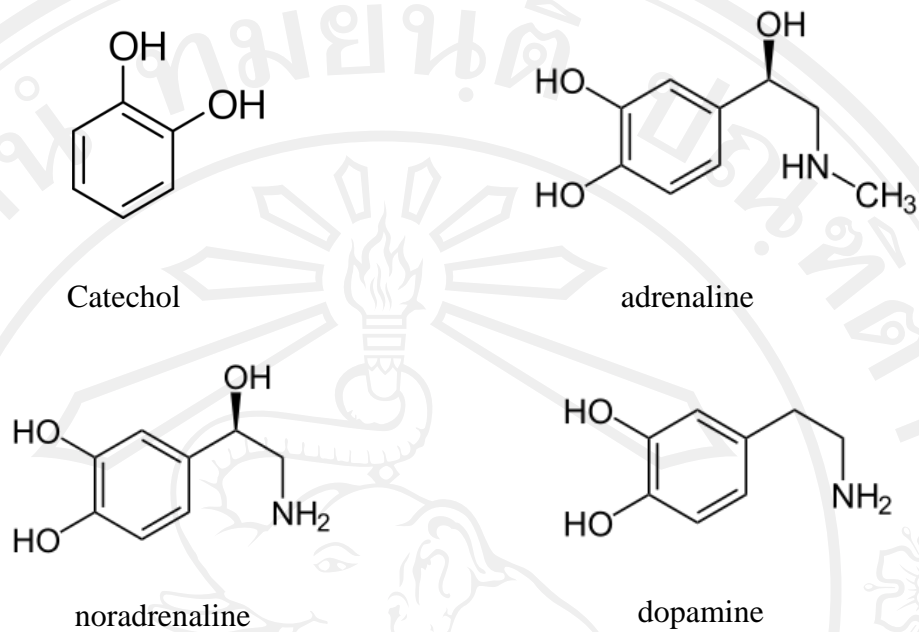


**Figure 1.16** Chemical structure of catechol and catecholamines [45].

Tyrosine is created from phenylalanine by hydroxylation via the enzyme phenylalanine hydroxylase as shown in Figure 1.17. Tyrosine is also ingested directly from dietary protein. It is then sent to catecholamine-secreting neurons. Here, several reactions serially convert tyrosine to L-DOPA, to dopamine, to norepinephrine, and eventually to epinephrine [48]. Various stimulant drugs are catecholamine analogues.

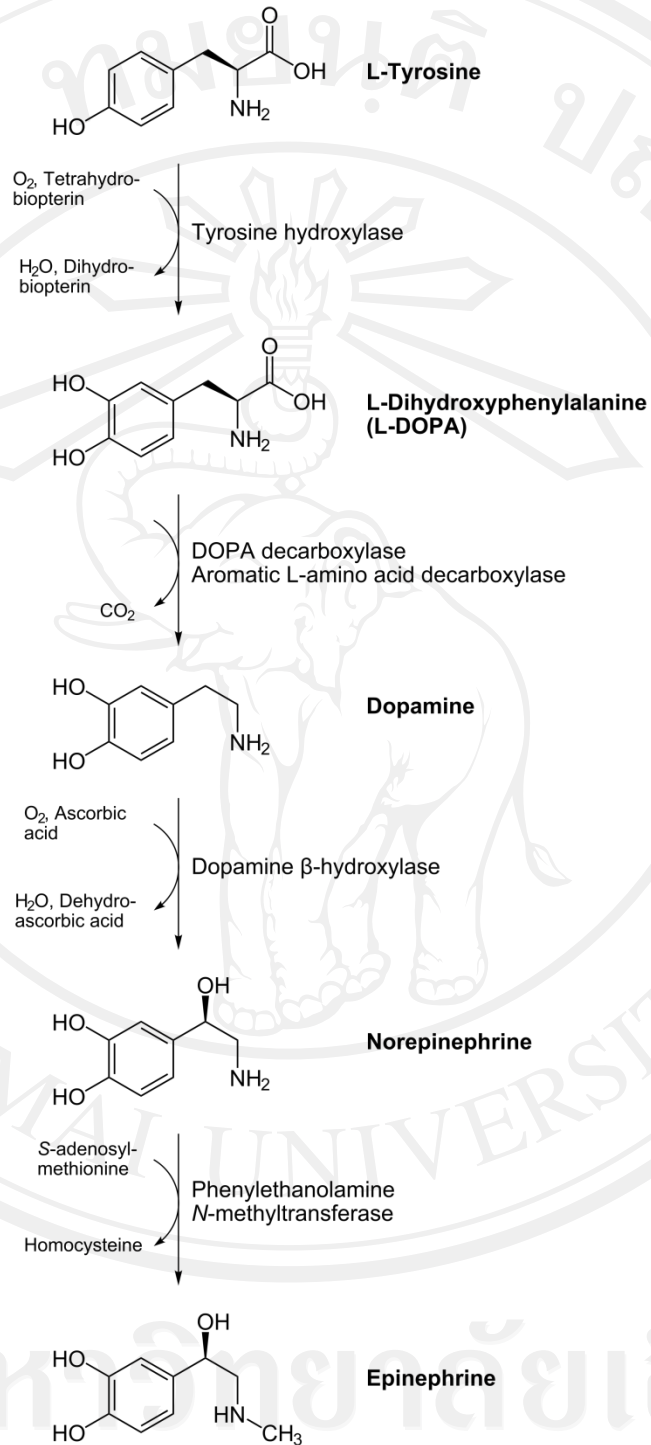


**Figure 1.17** Synthesis of catecholamines (adrenaline, noradrenaline, dopamine)

from tyrosine [48].

Two catecholamines, norepinephrine and dopamine, act as neuromodulators in the central nervous system and as hormones in the blood circulation. The catecholamine norepinephrine is a neuromodulator of the peripheral sympathetic nervous system but is also present in the blood (mostly through "spillover" from the synapses of the sympathetic system). High catecholamine levels in blood are associated with stress, which can be induced from psychological reactions or environmental stressors such as elevated sound levels, intense light, or low blood sugar levels. Extremely high levels of catecholamines (also known as catecholamine toxicity) can occur in central nervous system trauma due to stimulation and/or damage of nuclei in the brain stem, in particular those nuclei affecting the sympathetic nervous system. In emergency medicine, this occurrence is widely known as catecholamine dump. Extremely high levels of catecholamine can also be caused by neuroendocrine tumors in the adrenal medulla, a treatable condition known as pheochromocytoma. High levels of catecholamines can also be caused by monoamine oxidase A (MAO-A) deficiency. MAO-A is one of the enzymes responsible for degradation of these neurotransmitters, thus its deficiency increases the bioavailability of them considerably. It occurs in the absence of pheochromocytoma, neuroendocrine tumors, and carcinoid syndrome, but it looks similar to carcinoid syndrome such as facial flushing and aggression [49, 50].

Catecholamines cause general physiological changes that prepare the body for physical activity (fight or flight response). Some typical effects are increasing in heart rate, blood pressure, blood glucose levels, and a general reaction of the sympathetic nervous system. Some drugs, like tolcapone, raise the levels of all catecholamines.

#### 1.4.2 Adrenaline [51–53]

Adrenaline is a hormone produced by the adrenal glands during high stress or exciting situations. This powerful hormone is part of the human body's acute stress response system, also called the "fight or flight" response. It works by stimulating the heart rate, contracting blood vessels, and dilating air passages, all of which work to increase blood flow to the muscles and oxygen to the lungs. Additionally, it is used as a medical treatment for some potentially life-threatening conditions including anaphylactic shock. In the US, the medical community largely refers to this hormone as epinephrine, although the two terms may be used interchangeably [51].

The adrenal glands are found directly above the kidneys in the human body, and are roughly 3 inches (7.62 cm) in length. Adrenaline is one of several hormones produced by these glands. Along with norepinephrine and dopamine, it is a catecholamine, which is a group of hormones released in response to stress. These three hormones react with various body tissues, preparing the body to react physically to the stress causing situation.

The term "fight or flight" is often used to characterize the body's reaction to very stressful situations [52]. It is an evolutionary adaptation that allows the body to react to danger quickly. Dilated air passages, for example, allow the body to get more oxygen into the lungs quickly, increasing physical performance for short bursts of time. The blood vessels contract in most of the body, which redirects the blood toward the heart, lungs, and major muscle groups to help fuel their action.

When a person encounters a potentially dangerous situation, the hypothalamus in the brain signals the adrenal glands to release adrenaline and other hormones directly into the blood stream. The body's systems react to these hormones within seconds,

giving the person a nearly instant physical boost. Strength and speed both increase, while the body's ability to feel pain decreases. This hormonal surge is often referred to as an "adrenaline rush".

In addition to a noticeable increase in strength and performance, this hormone typically causes heightened awareness and increased respiration. The person may also feel lightheaded, dizzy, and experience changes in vision. These effects can last up to an hour, depending on the situation. When there is stress but no actual danger, a person can be left feeling restless and irritable. This is partly because adrenaline causes the body to release glucose, raising blood sugar, and giving the body energy that has no outlet. Many people find it beneficial to "work off" the adrenaline rush after a particularly stressful situation. In the past, people handled this naturally through fighting or other physical exertion, but in the modern world, high-stress situations often arise that involve little physical activity. Exercise can use up this extra energy.

Though adrenaline can play a key role in the body's survival, it can also cause detrimental effects over time. Prolonged and heightened levels of the hormone can put enormous pressure on the heart muscle and can, in some cases, cause heart failure. Additionally, it may cause the hippocampus to shrink. High levels of adrenaline in the blood can lead to insomnia and jittery nerves, and are often an indicator of chronic stress.

First synthesized in 1904, adrenaline is a common treatment for anaphylaxis, also known as anaphylactic shock [53]. It can be quickly administered to people showing signs of severe allergic reactions, and some people with known severe allergies carry epinephrine auto-injectors in case of an emergency. For these individuals, dosage

should be assigned by a licensed medical professional in advance, and instructions should be given on how and where it should be administered.

Adrenaline is also one of the main drugs used to treat low cardiac output the amount of blood the heart pumps and cardiac arrest. It can stimulate the muscle and increases the person's heart rate. In addition, by concentrating blood in the vital organs, including the heart, lungs, and brain, it helps increase the chances that the person will recover more fully.

#### 1.4.3 Uric acid [54–58]

Uric acid (UA) is a heterocyclic compound of carbon, nitrogen, oxygen, and hydrogen with the formula  $C_5H_4N_4O_3$  as Figure 1.18. It forms ions and salts known as urates and acid urates such as ammonium acid urate. UA is a product of the metabolic breakdown of purine nucleotides. High blood concentrations of UA can lead to a type of arthritis known as gout. The chemical is associated with other medical conditions including diabetes and the formation of ammonium acid urate kidney stones.

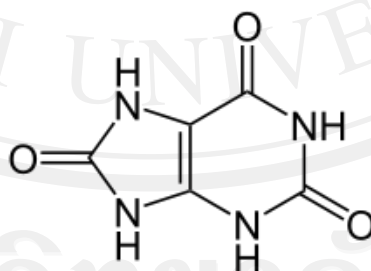


**Figure 1.18** Chemical structure of uric acid.

In human blood plasma, the reference range of UA is between 3.6 mg/dL (~214  $\mu\text{mol/L}$ ) and 8.3 mg/dL (~494  $\mu\text{mol/L}$ ) (1 mg/dL = 59.48  $\mu\text{mol/L}$ ), and 2.3–6.6 mg/dL for woman (137–393  $\mu\text{mol/L}$ ) [54]. This range is considered normal by the

American Medical Association Manual of Style [55]. UA concentrations in blood plasma above and below the normal range are known, respectively, as hyperuricemia and hypouricemia. Similarly, UA concentrations in urine above and below normal are known as hyperuricosuria and hypouricosuria. Such abnormal concentrations of UA are not medical conditions, but are associated with a variety of medical conditions.

Excess serum accumulation of UA in the blood can lead to a type of arthritis known as gout. This painful condition is the result of needle-like crystals of UA precipitating in joints, capillaries, skin, and other tissues. Kidney stones can also form through the process of formation and deposition of sodium urate microcrystals. A study found that men who drank two or more sugar-sweetened beverages a day have an 85% higher chance of developing gout than those who drank such beverages infrequently. Gout can occur where serum UA levels are as low as 6 mg/dL ( $\sim 357 \mu\text{mol/L}$ ), but an individual can have serum values as high as 9.6 mg/dL ( $\sim 565 \mu\text{mol/L}$ ) and not have gout [56].

Saturation levels of UA in blood may result in one form of kidney stones when the urate crystallizes in the kidney. These UA stones are radiolucent and so do not appear on an abdominal plain X-ray, and thus their presence must be diagnosed by ultrasound for this reason. Very large stones may be detected on X-ray by their displacement of the surrounding kidney tissues. UA stones, which form in the absence of secondary causes such as chronic diarrhea, vigorous exercise, dehydration, and animal protein loading, are felt to be secondary to obesity and insulin resistance seen in metabolic syndrome. Increased dietary acid leads to increased endogenous acid production in the liver and muscles, which in turn leads to an increased acid load to the kidneys. This load is handled more poorly because of renal fat infiltration and

insulin resistance, which are felt to impair ammonia excretion (a buffer). The urine is therefore quite acidic, and UA becomes insoluble, crystallizes and stones form. In addition, naturally present promoter and inhibitor factors may be affected. This explains the high prevalence of uric stones and unusually acidic urine seen in patients with type 2 diabetes. UA crystals can also promote the formation of calcium oxalate stones, acting as "seed crystals" (heterogeneous nucleation) [57].

UA has been successfully used in the treatment and prevention of the animal (murine) model of MS. A 2006 study found elevation of serum UA values in multiple sclerosis patients, by oral supplementation with inosine, resulted in lower relapse rates, and no adverse effects [58].

#### 1.4.4 Ascorbic acid [59, 60]

Ascorbic acid (AA) is a naturally occurring organic compound with antioxidant properties. It is a white solid, but impure samples can appear yellowish. It dissolves well in water to give mildly acidic solutions. AA is one form ("vitamer") of vitamin C. It was originally called L-hexuronic acid, but when it was found to have vitamin C activity in animals ("vitamin C" being defined as a vitamin activity, not then a specific substance), the suggestion was made to rename L-hexuronic acid. The new name for L-hexuronic acid is derived from  $\alpha$ - (meaning "no") and scorbutus (scurvy), the disease caused by a deficiency of vitamin C. Because it is derived from glucose, many animals are able to produce it, but humans require it as part of their nutrition.

Other vertebrates lacking the ability to produce AA include other primates, guinea pigs, teleost fishes, bats, and birds, all of which require it as a dietary micronutrient (that is, a vitamin) [59].

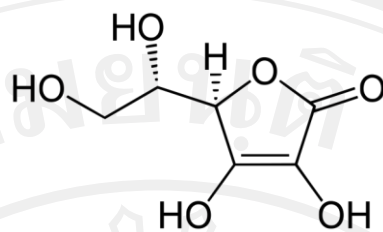


**Figure 1.19** Chemical structure of ascorbic acid.

Chemically, there exists a D-ascorbic acid which does not occur in nature. It may be synthesized artificially. It has identical antioxidant properties to L-ascorbic acid (as shown in Figure 1.19), yet has far less vitamin C activity (although not quite zero) [60]. This fact is taken as evidence that the antioxidant properties of AA are only a small part of its effective vitamin activity. Specifically, L-ascorbate is known to participate in many specific enzyme reactions which require the correct primer (L-ascorbate and not D-ascorbate).

As a mild reducing agent, AA degrades upon exposure to air, converting the oxygen to water. The redox reaction is accelerated by the presence of metal ions and light. It can be oxidized by one electron to a radical state or doubly oxidized to the stable form called dehydroascorbic acid.

Ascorbate usually acts as an antioxidant. It typically reacts with oxidants of the reactive oxygen species, such as the hydroxyl radical formed from hydrogen peroxide. Such radicals are damaging to animals and plants at the molecular level due to their possible interaction with nucleic acids, proteins, and lipids. Sometimes these radicals initiate chain reactions. Ascorbate can terminate these chain radical reactions by electron transfer. AA is special because it can transfer a single electron, owing to the

stability of its own radical ion called "semi-dehydroascorbate", dehydroascorbate as shown in Figure 1.20. The net reaction is:



The oxidized forms of ascorbate are relatively unreactive, and do not cause cellular damage. However, being a good electron donor, excess ascorbate in the presence of free metal ions can not only promote but also initiate free radical reactions, thus making it a potentially dangerous pro-oxidative compound in certain metabolic contexts.

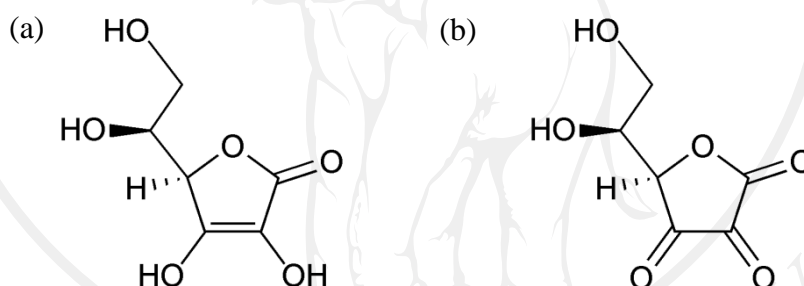


**Figure 1.20** Chemical structure of (a) ascorbic acid (reduced form of Vitamin C) and (b) dehydroascorbic acid (oxidized form of Vitamin C).

Dehydroascorbic acid (DHA) is the oxidized form of AA. Both DHA and AA are important compounds in various dietary components. DHA has stronger antiviral effect and different mechanism of action than ascorbic acid.

### 1.5 Single-wall carbon nanotubes (SWNTs) [61–67]

Carbon nanotubes (CNTs), consist of sheet of graphite rolled into cylinder. There are two groups of carbon nanotubes, multi-wall carbon nanotubes (MWNTs) and single-wall carbon nanotubes (SWNTs) [61]. The MWNTs consist of several layers of

graphite sheets rolled into cylinders with one cylinder inside another and SWNTs consist of a single graphite sheet rolled seamlessly, defining a cylinder of 1-2 nm diameter. Theoretical calculations have predicted that this material will behave either as a metal or semiconductor depending on its size and lattice helicity. SWNTs have low resistivity of 100–200  $\mu\Omega \cdot cm$  comparable with a high-quality carbon fiber with a resistivity of approximately 100  $\mu\Omega \cdot cm$  [62]. The SWNTs can carry electrical current densities up to 109 A/cm<sup>2</sup> and remain stable at high temperature in the chemical reaction.

Single-walled nanotubes (SWNTs) have a diameter of close to 1 nanometer, with a tube length that can be many millions of times longer [63]. The structure of a SWNT can be conceptualized by wrapping a one-atom-thick layer of graphite called graphene into a seamless cylinder. The way the graphene sheet is wrapped is represented by a pair of indices ( $n, m$ ). The integers  $n$  and  $m$  denote the number of unit vectors along two directions in the honeycomb crystal lattice of graphene. If  $m = 0$ , the nanotubes are called zigzag nanotubes, and if  $n = m$ , the nanotubes are called armchair nanotubes. Otherwise, they are called chiral as shown in Figure 1.21 [63].

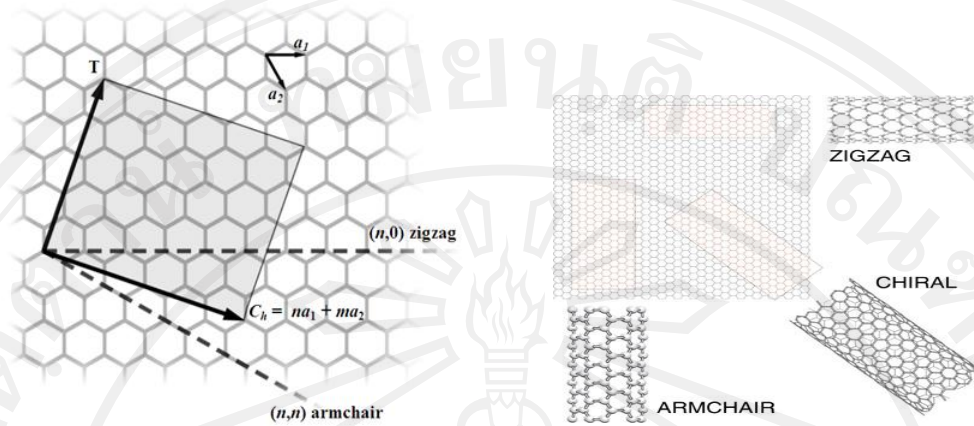


**Figure 1.21** Tube chirality explained on graphene sheet and the graphite sheet is rolled into a nanotube [63].

The diameter of an ideal nanotube can be calculated from its  $(n, m)$  indices as follows:

$$d = \frac{a}{\pi} \sqrt{(n^2 + nm + m^2)} \quad 1.9$$

where  $a = 0.246$  nm. SWNTs are an important variety of carbon nanotube because most of their properties change significantly with the  $(n, m)$  values, and this dependence is non-monotonic (see Kataura plot in Figure 1.22 [63]). A nanotube of certain diameter can be metallic M or semiconducting S; it can have several band gaps, conventionally labeled as  $S_{11}$ ,  $S_{22}$ ,  $M_{11}$ ,  $M_{22}$ , etc.

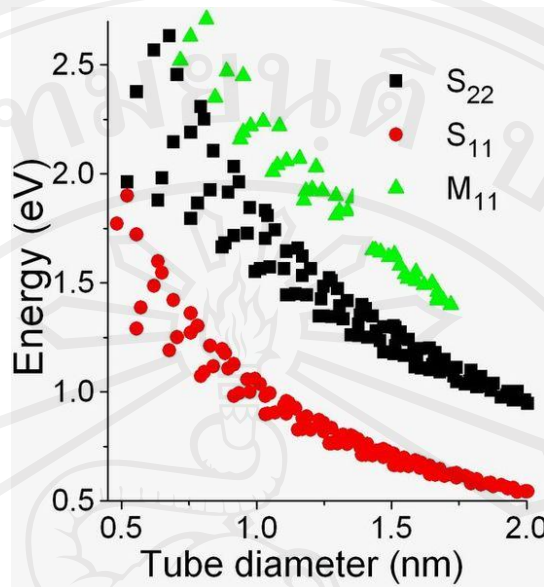


**Figure 1.22** Kataura plot of the energy of an electronic transition decreases as the diameter of the nanotube increases [63].

In particular, their band gap can vary from zero to about 2 eV and their electrical conductivity can show metallic or semiconducting behavior. Single-walled nanotubes are likely candidates for miniaturizing electronics. The most basic building block of these systems is the electric wire, and SWNTs with diameters of an order of a nanometer can be excellent conductors [64, 65]. One useful application of SWNTs is in the development of the first intermolecular field-effect transistors (FET). The first intermolecular logic gate using SWNT FETs was made in 2001 [66]. A logic gate requires both a p-FET and an n-FET. Because SWNTs are p-FETs when exposed to oxygen and n-FETs otherwise, it is possible to protect half of an SWNT from oxygen exposure, while exposing the other half to oxygen. This results in a single SWNT that acts as a NOT logic gate with both p and n-type FETs within the same molecule.

The intrinsic mechanical and transport properties of carbon nanotubes make them the ultimate carbon fibers. The following tables (Table 1.3 and Table 1.4) compare physical and electrical properties to other engineering materials.

Overall, carbon nanotubes show a unique combination of stiffness, strength, and tenacity compared to other fiber materials which usually lack one or more of these properties. Thermal and electrical conductivity are also very high, and comparable to other conductive materials.

**Table 1.3** Mechanical properties of engineering fibers [67]

Fiber Material	Specific Density	E (TPa)	Strenght (GPa)	Strain at Break (%)
Carbon Nanotube	1.3–2	1	10–60	10
HS Steel	7.8	0.2	4.1	< 10
Carbon Fiber - PAN	1.7–2	0.2–0.6	1.7–5	0.3–2.4
Carbon Fiber - Pitch	2–2.2	0.4–0.96	2.2–3.3	0.27–0.6
E/S - glass	2.5	0.07/0.08	2.4/4.5	4.8
Kevlar* 49	1.4	0.13	3.6–4.1	2.8

Kevlar is a registered trademark of DuPont product.

**Table 1.4** Transport properties of conductive materials [67]

Material	Thermal Conductivity (W/m.k)	Electrical Conductivity
Carbon Nanotubes	> 3000	10 <sup>6</sup> –10 <sup>7</sup>
Copper	400	6 x 10 <sup>7</sup>
Carbon Fiber - Pitch	1000	2–8.5 x 10 <sup>6</sup>
Carbon Fiber - PAN	8–105	6.5–14 x 10 <sup>6</sup>

#### Potential Applications for Carbon Nanotubes[67]

Carbon Nanotube Technology can be used for a wide range of new and existing applications as follows:

- Conductive plastics
- Structural composite materials
- Flat-panel displays
- Gas storage
- Antifouling paint
- Micro- and nano-electronics
- Radar-absorbing coating
- Technical textiles
- Ultra-capacitors
- Atomic Force Microscope (AFM) tips
- Batteries with improved lifetime
- Biosensors for harmful gases
- Extra strong fibers

### 1.6 ZnO nanoparticles [68–78]

ZnO nanoparticles have been mostly synthesized through wet-chemical methods such as precipitation [68], sol-gel [69] and hydrothermal [70] syntheses. Additionally, ZnO has been obtained in film form through techniques including pulsed laser deposition [71], sol-gel dip-coating [72], magnetron sputtering [73]. Various workers have been working on synthesis and characterization of different nanostructures of pure and doped zinc oxide. Spanhel and Anderson [74] have explained the synthesis of nanocrystals of zinc oxide using distillation set-up starting with products of zinc acetate and ethanol. Using this technique they have obtained highly concentrated colloidal nanocrystals of ZnO of size varying from 3.5–5.5 nm with ageing and shown that these crystals remain in a dispersed state for weeks. Hossain et al. [75] had further modified this technique successfully to obtain nanobelts of ZnO of length 700  $\mu\text{m}$  using refluxing technique.

Nanocrystalline ZnO using  $\text{ZnCl}_2 \cdot 2\text{H}_2\text{O}$  and  $(\text{NH}_4)_2\text{CO}_3$  as raw materials by direct precipitation method was reported by Siqingaowa et al. [76]. The nanocrystalline ZnO was characterized using XRD, TEM and BET. Experimental results for nanocrystalline ZnO showed that the minimum size was about 8 nm, the maximum was about 15 nm and the mean grain size was 12 nm, the surface area was  $80.56 \text{ m}^2/\text{g}$  and the purity was 99.9% when the precursor was calcined at  $300 \text{ }^\circ\text{C}$  for 2 hr.

Nanocrystalline ZnO powders have been synthesized by means of a novel gel-network precipitation method using gelatin as a template at lower temperature condition were reported by Zhou et al. [77]. The products were characterized by using TG-DTA, XRD and TEM techniques. The products appeared to be regularly spherical

or elliptical and their sizes range from 20 to 40 nm. The average particle size increased with increasing calcining temperature, and decreased with increasing gelatin concentration. Furthermore, the photoluminescence (PL) spectra of the ZnO nanopowders were also investigated. The relative luminescent intensities for the ultraviolet band and green emission band showed a dependence on preparation conditions.

Hydrothermal process was applied to synthesize zinc oxide nanocrystals by Chen et al. [70]. X-ray powder diffraction and scanning electron microscopy were used to analyze the crystal structure and surface morphology. XRD pattern analysis showed that the ZnO clusters are single hexagonal phase of wurtzite structure (space group P63mc) with no impurity of Zn and Zn(OH)<sub>2</sub>. Also, SEM images revealed that the size of a single ZnO crystal is between 200–500 nm in diameter and 2–5 μm in length.

Burunkaya et al. [78] synthesized aluminum doped zinc oxide (AZO) nanometric particles by hydrothermal method. Aluminum nitrate hydrate, aluminum sec-butoxide and zinc nitrate hydrate were used as the starting materials, and n-propanol and 2-butanol were used as solvents. Obtained products were subjected to powder-XRD, particle size measurement, TEM examination and AAS analysis. Single phase AZO particles were obtained at alcohol to zinc nitrate ratio of 35, acid to zinc nitrate ratio of 0.2, at 225 °C. Particle size was determined as  $3.2 \pm 0.4$  nm from TEM examinations and as 1–2 nm from dynamic light scattering.

Liewhiran et al. [94] synthesized ZnO nanoparticles by flame spray pyrolysis using zinc naphthenate as a precursor dissolved in toluene/acetonitrile (80/20 vol%). The particles properties were analyzed by XRD, BET. The ZnO particle size and morphology was observed by SEM and HR-TEM revealing spheroidal, hexagonal,

and rod-like morphologies. The crystallite sizes of ZnO spheroidal and hexagonal particles ranged from 10–20 nm. ZnO nanorods were ranged from 10–20 nm in width and 20–50 nm in length. Sensing films were produced by mixing the nanoparticles into an organic paste composed of terpineol and ethyl cellulose as a vehicle binder.

### 1.7 Literature review

Conducting polymers (CPs) have received considerable attention because of their electronic conducting properties and unique chemical and biochemical properties. CPs are materials discovered just over 20 years ago which have aroused considerable interest on account of their electronic conducting properties and unique chemical and bio-chemical properties [1, 28–30].

In 1996, liquid chromatographic (LC) method with 2-phenylcinonitrile (PGN) and benzylamine (BA) were successfully applied to the determination of CA in human urine was reported by Notha et al [88]. The PGN and BA reagent were the suitable reagents in terms of selectivity and sensitivity with catecholamines under mild conditions in the presence of ammonium molybdate and sodium periodate for PGN and potassium hexanoferrate (III) for BA to give fluorescent derivatives. The derivatives of adrenaline, noreadrenaline and dopamine could be separated within 13 min by reversed phase liquid chromatography with isocratic elution and measured fluorimetrically as described above. The detection limit ( $S/N = 3$ ) were in the range 5.2–11 fmol for PGN and 1.6–100 fmol for BA in a 50  $\mu\text{L}$  injection volume.

In 1998, contributions summarize the use of plasmon surface polaritons and guided optical waves for the characterization of interfaces and thin organic films were as reported by Knoll et al. [39]. The interfacial “light” can be employed to monitor thin coatings at a solid/air or solid/liquid interface. Examples were given for a very sensitive thickness determination of samples ranging from self-assembled monolayer, to multilayer assemblies prepared by the Langmuir/Blodgett/Kuhn technique or by the alternate polyelectrolyte deposition. These were complemented by the demonstration of the potential of the technique to also monitor time dependent processes in a kinetic mode.

In 2001, electrochemical oxidation/reduction and the transition in the conductivity of polyaniline (PANI) film on gold electrode surface were reported by Kang et al. [85]. Based on the amplification response of SPR to the redox transformation of PANI film as a direct result of the enzymatic reaction between horseradish peroxidase (HRP) and PANI in the presence of  $H_2O_2$ . The novel PANI-mediated HRP sensor has been fabricated of SPR biosensor because the other oxidoreductases can all be used as immobilization enzyme to transform PANI film. The SPR biosensor posed a number of potential advantages. First, a larger SPR signal could be obtained in the SPR measurement than in the direct binding assay of SPR. Second, the SPR measurement did not require electrochemical instrument to operate.

In 2003, CPs were reported by Vidal et al. [28] with numerous (bio)analytical and technological applications. CPs are easily synthesized and deposited onto the conductive surface of a given substrate from monomer solutions by electrochemical polymerization with precise electrochemical control of their formation rate and

thickness. Coating electrodes with CPs under mild conditions opens up enormous possibilities for the immobilization of biomolecules and bioaffinity or biorecognizing reagents, improve of their electrocatalytic properties, rapid electron transfer and direct communication to produce a range of analytical signals and new analytical applications. CPs still has many unexplored possibilities, and so a lot of future research into the development of new CP-based biosensors can be expected.

In 2003, combination of SPR and surface plasmon enhanced photoluminescence spectroscopy (SPPL) with electrochemical techniques for the detection of photoluminescence in poly(3,4-ethylenedioxythiophene) (PEDOT) ultrathin films were reported by Baba and Knoll [81]. The photoluminescence from PEDOT was detected when the polymer was dedoped under the influence of the corresponding applied potential. The photoluminescence intensity was controlled by the potential and was dependent on the angular position in an SPR reflectivity experiment. The SPR characterization of the PEDOT film was consistent with the PEDOT bulk electrochromic properties obtained from UV-vis-NIR spectra. A mechanistic model of the photoluminescence from PEDOT was obtained by taking into consideration the reflectivity and the SPPL data, which could be observed simultaneous by their system.

In 2003, MWNTs film-coated glassy carbon electrode (GCE) exhibited a marked enhancement effect on the current response of dopamine (DA) and serotonin (5-HT) and lowers oxidation over potentials were reported by Wu et al. [89]. The results confirmed that the Nafion–MWNTs modified disk form CFME possesses the obvious advantage of easy preparation in a rapid and simple procedure, effective electrocatalytic properties, and very low detection limits for DA, even in the presence

of a 100 to 1000-fold excess of AA. The combination of the good electrical properties of MWNTs with the negatively charged polymer of Nafion on the carbon fiber micro electrode surface has realized an efficient electrochemical microsensor capable of maintaining reproducibility and stability. The resulting technique can be used to monitor DA concentrations at nM levels in micro-volume samples.

In 2003, poly(acridine red) modified glassy carbon electrode was used for the detection of dopamine in the presence of AA in a pH 7.4 phosphate buffer solutions (PBS) by cyclic voltammetry and differential pulse voltammetry were reported by Zhang et al. [90]. The electrode was disposed by cyclic sweeping from  $-1.0$  to  $+2.5$  V at  $100 \text{ mV s}^{-1}$  for 10 circles in pH 7.4 PBS containing  $1.0 \times 10^{-4} \text{ mol dm}^{-3}$  acridine red solution. The poly(acridine red) film modified electrode could promote DA oxidation. Peak current of DA was proportional to the concentration over the range of  $1.0 \times 10^{-7} \sim 1.0 \times 10^{-4} \text{ mol dm}^{-3}$  with a detection limit ( $S/N = 3$ ) of  $1.0 \times 10^{-9} \text{ mol dm}^{-3}$ . AA had hardly interference with the determination of dopamine. The proposed method exhibited good recovery and reproducibility.

In 2004, Polymers have gained tremendous recognition in the field of artificial sensor with the goal of mimicking natural sense organs. Better selectivity and rapid measurements have been achieved by replacing classical sensor materials with polymers involving nanotechnology and exploiting either the intrinsic or extrinsic functions of polymers. Semiconductors, semiconducting metal oxides, solid electrolytes, ionic membranes, and organic semiconductors have been the classical materials for sensor devices. Polymers with sensing behavior were reported by

Adhikari and Majumdar [29] through modification of the polymer by functionalization.

In 2004, the electropolymerization and doping/dedoping properties of polyaniline ultrathin films on Au electrode surfaces were investigated by Baba et al. [23] using EC-SPR and the electrochemical quartz crystal microbalance (EC-QCM). Surface plasmons are excited by reflecting p-polarized laser light off the Au-coated base of the prism. The excitation sources employed were two different He–Ne lasers:  $\lambda = 632.8$  and 1152 nm. Kinetic measurements were performed in order to monitor the formation of the PANI film and the oxidation/reduction and doping/dedoping properties of the deposited PANI thin film via reflectivity changes as a function of time. The real and imaginary parts of the dielectric constant of the PANI thin film at several doping levels was determined quantitatively by taking into consideration the thickness values obtained from the EC-QCM measurement. The combination of these two techniques provides a powerful method for probing the electrical, optical, and dielectric properties of conjugated ultrathin polymer films.

In 2006, electroactive polymers such as polypyrrole (PPy) were used as coating for electrodes or neural probes and as scaffolds to induce tissue regeneration by Lee et al. [30]. Acid functionalized PPy substituted at the N-position, poly(1-(2-carboxyethyl)pyrrole) (PPyCOOH), was demonstrated as a bioactive platform for surface modification and cell attachment. PPyCOOH films were prepared by electrochemical polymerization of 1-(2-carboxyethyl)pyrrole monomer that was synthesized from 1-(2-cyanoethyl)pyrrole. Human umbilical vascular endothelial cells (HUVECs) cultured on PPyCOOH films surface-modified with the cell adhesive Arg–

Gly–Asp (RGD) motif demonstrated improved attachment and spreading. Thus, PPyCOOH could be useful in developing PPy composites that contain a variety of biological molecules as bioactive conducting platforms for specific biomedical purposes.

In 2006, SPR technique was reported by Damos et al. [79] to monitor the electropolymerization and doping/dedoping processes of thin polypyrrole films on flat gold surfaces. The changes in the electrochemical and optical properties of the thin polypyrrole films upon applying potential sweeps produced a significant change in the SPR angle position due to changes in the real and imaginary parts of the complex dielectric constant during doping/dedoping processes, the doping and dedoping processes in the polypyrrole film can act directly on optical properties while the EC-SPR technique can give the same information indirectly.

In 2007, the specific information of CPs was provided on their modification for use in applications such as biosensors, tissue engineering, and neural probes were reported by Guimard et al. [1]. This was especially true in biomedicine, where many applications benefit from the presence of conductive materials, whether for biosensing or for control over cell proliferation and differentiation.

In 2008, EC-SPR measurement used for in situ monitoring the formation of polypyrrolepropylic acid (PPA) film was report by Dong et al. [80]. Further precise control of the film thickness for tailor the film for an optimized architecture of an immunosensor was performed. 0.3 M PPA monomer in 0.1 M phosphate buffer saline (PBS) solution was used for electropolymerization of PPA film on gold surface, which was conducted by cyclic voltammetry in a range from  $-0.3$  to  $0.75$  V versus

SCE. Specifically, 150  $\mu\text{L}$  above mentioned solutions were added into the cuvette and the SPR baseline was recorded for several minutes until the SPR angle became stable. The calibration curves of EC-SPR measurement exhibited a similar dependence on the bulk concentration of antigen. An approximate linear relationship could be obtained by plotting the data in semi-logarithmic reference frame compared with EC-SPR showed higher sensitivity with prolonged time.

In 2008, SPR was employed to study protein immobilization on poly(pyrrole-co-pyrrolepropylic acid) (PPy/PPa) for immunosensing applications by Hu et al. [83]. SPR was employed to in situ monitor the electropolymerization process and to control thickness of the PPy/PPa copolymer film. Goat IgG as a model protein was covalently immobilized on the carboxyl containing film through ethyl(dimethylaminopropyl) carbodiimide/N-hydroxysuccinimide (EDC/NHS) as the coupling reagents. The effect of pyrrolepropylic acid (Pa) proportion in the deposition solution on the protein immobilization capability was systemically investigated. The immobilization efficiency was demonstrated by a label-free SPR immunosensor.

In the same year of 2008, SPR method was employed bilayer lipid membrane (BLM) based on immobilizing horseradish peroxidase (HRP) in the BLMs supported by the redox polyaniline (PANI) film to detect enzymatic reaction by Wang et al. [84]. SPR kinetic curve in situ monitoring the redox transformation of PANI film resulted from the reaction between HRP and PANI. The enzymatic reaction of HRP with  $\text{H}_2\text{O}_2$  was successfully analyzed by electrochemical SPR spectroscopy. The results showed that this BLM supported on PANI film could not only preserve the bioactivity of HRP immobilized in the membrane, but also provide a channel for the

transfer of electrons between HRP and PANI on electrode surface. These characteristics enabled the development of SPR biosensor for sensitively detecting  $\text{H}_2\text{O}_2$ . The SPR sensor surface was completely regenerated by electrochemically reducing the oxidized PANI to its reduced state.

In 2008, selective DA determinations using porous-carbon-modified glassy carbon electrodes (GCE) in the presence of AA were reported by Song et al. [91]. The effects of structure textures and surface functional groups of the porous carbons on the electrochemical behavior of DA was analyzed based on both cyclic voltammetry (CV) and differential pulse voltammetry (DPV) measurements. The differential pulse voltammetry of DA on the modified GCE was determined in the presence of 400-fold excess of AA, and the linear determination ranges of 0.05–0.99, 0.20–1.96, and 0.6–12.60  $\mu\text{M}$  with the lowest detected concentrations of  $4.5 \times 10^{-3}$ ,  $4.4 \times 10^{-2}$ , and 0.33  $\mu\text{M}$  respectively were obtained on the mesoporous carbon, mesoporous carbon with carboxylic and amino groups modified electrodes.

In 2008, carbon fiber microelectrode (CFME) modified by Nafion and single-walled carbon nanotubes (SWNTs) was reported by Jeong and Jeon [92] using voltammetric methods for determination of DA in the presence of AA in phosphate buffer saline (PBS) solution at pH 7.4. The SWNTs have high surface area, good electrical properties and Nafion is a negatively charged polymer and surfactant, therefore composite of SWNTs and Nafion in the electrode film should promote the selectivity and sensitivity of DA detection in the presence of the interfering AA molecule. Voltammetric techniques separated the anodic peaks of DA and AA, the interference from AA was effectively excluded from DA determination. Dopamine

can be determined without any interference from AA at the modified microelectrode, thereby increasing the sensitivity, selectivity, and reproducibility and stability. The result of this technique can be used to monitor DA concentrations at nM levels in micro-volume samples.

In 2009, the attenuated total reflection (ATR) and emission light properties utilizing surface plasmon (SP) excitations were measured for the electrochemical change of poly(3-hexylthiophene-2,5-diyl) (P3HT) thin films in situ by Kato et al. [82]. The SP emission light could detect the SP excited by molecular luminescence of P3HT. SPs were excited at the metal dielectric interface, upon total internal reflection of polarized light from a He–Ne laser with the wavelength of 632.8 nm. The optical/electrochemical process at the Au thin film was detected by monitoring the reflectivity as a function of the incident angle. The SP emission light was obtained by the irradiation of Ar<sup>+</sup> laser beam with the wavelength of 488.0 nm. The P3HT thin film was luminous upon the light irradiation, and excited SP emission light was measured. The SP emission light also decreased by decrease of the molecular luminescence of P3HT by the doping. For the dedoped-state P3HT thin films, the SP emission light also increased with increase of the molecular luminescence. The ATR and SP emission light properties were remarkably changed with the doping and dedoping. The reversible change of the SP emission light was observed by the doping and the dedoping. The SP emission light excited by molecular luminescence can be controlled by the control of doping-dedoping state.

In 2009, cation surfactant cetyltrimethyl ammonium bromide (CTAB) modified carbon paste electrode (CPE) was reported by Shankar et al. [86] for simultaneous

determination of AA, DA and UA. The CPE was prepared as follows, 70% graphite powder and 30% silicone oil were mixed by hand in an agate mortar to produce a homogeneous paste. The paste was then packed into the cavity of a homemade CPE and smoothed on a weighing paper. CTAB modified CPE (CTABMCPE) was prepared by immobilizing the CTAB solution on to the surface of bare CPE. CTABMCPE strongly enhanced both anodic and cathodic peak current of DA. The increase in the concentration of DA resulted in greater the enhancement of electrochemical oxidation at certain stage. Electrochemical process was found to be adsorption controlled and the results also indicated that the problem of the overlapped voltammetric responses of DA with AA and UA, due to their co-existence in real biological matrixes could be effectively overcome by the use of CTABMCPE the modified electrode which has a good selectivity, sensitivity and reproducibility.

In 2010, electrochemical system was fabricated using layer by layer (LbL) technique on graphite electrode, by positively charged poly(diallyldimethylammonium chloride) (PDDA) and negatively charged MWCNTs wrapped with poly styrene sulfonate (PSS) through electrostatic interaction, for the simultaneous determination of AA, DA and UA were reported by Manjunatha et al. [87]. Solubility of MWNTs in water was increased by using linear polymer PSS. The PSS wrapped MWCNTs modified electrodes were characterized by electrochemical impedance spectroscopy (EIS), cyclic voltammetry (CV) and differential pulse voltammetry (DPV) and chronoamperometric techniques. The modified electrode exhibits superior electrocatalytic activity towards AA, DA and UA than the bare graphite electrode. No electrode fouling was observed during all the

experiments and good stability and reproducibility was obtained for simultaneous determination of AA, DA and UA.

In 2010, poly(3-aminobenzylamine) (P3ABA) prepared by electropolymerization of 3-aminobenzylamine on gold-coated glass electrode, which specific reaction of benzylamine within the P3ABA structure with adrenaline was reported by Baba et al. [6]. Adrenaline was detected in real time by EC-SPR spectroscopy, which provides simultaneous monitoring of both optical and current response upon injection of adrenaline into P3ABA film. Furthermore, UV-vis spectroscopy and XPS were studied the reaction of adrenaline with the PABA film. UV-vis spectra at 320 nm increased and 410 nm diminished after injection of adrenaline were changed, which suggest that the chemical structure of the PABA film had changed as a result of the reaction with adrenaline. The  $-\text{NH}_3^+$  bonds decreased from 49.0 to 20.3%,  $-\text{N}=\text{}$  bonds were measured from 7.2 to 22.1% and the increased in the  $-\text{NH}-$  bond from 20.9 to 49.1% in XPS results, which suggested that the reaction of adrenaline into PABA film included specific the reaction from benzylamine site and physical adsorption. The EC-SPR reflectivity response of UA and AA showed interference smaller than the reflectivity change in adrenaline because of non-specific reaction with PABA thin film. The number of changes in both current and SPR reflectivity on the injection of adrenaline exhibited the linear relation to the concentration and the detection limit was 100 pM.

In 2010, a glassy carbon electrode modified with single wall carbon nanotubes (SWNTs/GC) for electrochemical determination of dopamine was reported by Chuekachang et al. [93] using cyclic voltammetry (CV) and differential pulse

voltammetry (DPV). The electrode was coated with 10  $\mu\text{L}$  of the black suspension of SWNT (1 mg/mL) in N,N-dimethylformamide (DMF) and heated under an infrared lamp to remove the solvent. The SWNTs/GC 10  $\mu\text{L}$  was used to test the linearity of anodic oxidation of dopamine by DPV. The peak current increased linearly with concentration of dopamine in the range of 2.5–25 ppm ( $R^2 = 0.9766$ ). For the life time of the SWNTs/GC, the cut-off criterion of the DPV was detected in the reduction of current by 50 %. The lifetime of the modified SWNTs depended on the oxidation of dopamine because of fouling of the electrode surface due to the adsorption of oxidation products, 34 repetition cycles was obtained. The detection limit of the dopamine as obtained from the oxidation current in DPV was 0.021 ppm ( $S/N = 3$ ) with minimum current for the detection of dopamine of 0.033  $\mu\text{A}$ . The reproducibility of electrocatalytic studies was better within 90% (10% RSD). The relative standard deviation (RSD) of 8.42% for 100 ppm dopamine ( $n = 20$ ) showed excellent reproducibility.

In 2011, poly(pyrrole-3-carboxylic acid) film constructed by electropolymerization of pyrrole-3-carboxylic acid monomer on gold-coated glass electrode for the detection of human immunoglobulin G was reported by Janmanee et al. [8]. In this research study the kinetic property and electroactivity property of the PP3C thin film by EC-SPR. The carboxylic acid surface of the PP3C film was activated for the immobilization of anti-human IgG, which have more space inside the polymer chain for the binding of anti-human IgG and human IgG. UV-vis spectroscopy was performed to characterize the PP3C thin film at a difference applied constant

potentials. Furthermore, AFM was performed to characterize the mechanism of improved sensitivity of immobilized human IgG.

Therefore, this study aims to fabricate poly(2-aminobenzylamine) (P2ABA) and P2ABA/SWNTs, P2ABA/ZnO nanoparticles composite thin films by EC-SPR spectroscopy for the detection of some biomolecules such as adrenaline, AA and UA. The P2ABA thin film will be employed to detect adrenaline because P2ABA thin film has a good electrical conductivity, environmental stability, ease to synthesis and stable at neutral solution. Furthermore, P2ABA has a benzylamine group in the structure which specifically reacts with adrenaline. P2ABA thin film formation on the gold-coated glass substrate will be evaluated by EC-SPR spectroscopy. The interaction between the adrenaline and the benzylamine within P2ABA structure on the gold-coated glass substrate will be detected in real time by a change in SPR reflectivity signal. Furthermore, the reaction of P2ABA thin film with adrenaline will be studied by UV-vis absorption spectroscopy, AFM, FT-IR/ATR and QCM-D techniques compared to the response interference detection of UA and AA. The QCM-D techniques will be employed to study the molecular interaction and adsorption between P2ABA thin film and adrenaline.

### **1.8 Research Objectives**

- 1.8.1 To fabricate the conducting polymer, the conducting polymer/SWNTs composites thin film by electrochemical-surface plasmon resonance (EC-SPR) spectroscopy
- 1.8.2 To characterize and study the properties of conducting polymer/SWNTs composites thin film using EC-SPR spectroscopy, UV-vis absorption spectroscopy, FTIR/ATR, AFM and QCM-D techniques.
- 1.8.3 To fabricate an electrochemical sensor based on the prepared films
- 1.8.4 To detect some biomolecules such as adrenaline, UA and AA using conducting polymer/SWNTs composite and conducting polymer/ZnO nanoparticles composite thin films

### **1.9 Usefulness of the Research (Theory and/or Applied)**

Novel conducting polymer/SWNTs composites thin film fabricated by EC-SPR will be obtained for the detection of some biomolecules (adrenaline, UA and AA).

### **1.10 Research plan, methodology and scope**

- 1.10.1 Literature review
- 1.10.2 Fabrication of conducting polymer, conducting polymer/SWNTs composite and conducting polymer/ZnO nanoparticles composite thin films by EC-SPR spectroscopy technique
- 1.10.3 Characterize and study the properties of conducting polymer/SWNTs composites thin film by using EC-SPR spectroscopy, UV-vis absorption spectroscopy, FT-IR/ATR, AFM and QCM-D

techniques

1.10.4 Fabrication of electrochemical sensor based on the prepared films

1.10.5 Detection of some biomolecules such as adrenaline, UA and AA, using conducting polymer/SWNTs composite and conducting polymer/ZnO nanoparticles composite thin films

1.10.6 Discussions and conclusion